Thermosensory behaviors of the free-living life stages of *Strongyloides* species support parasitism in tropical environments

Ben T. Gregory[1], Mariam Desouky[1], Jaidyn Slaughter[2], Elissa A. Hallem[3,4], Astra S. Bryant[1*]

[1] Department of Physiology and Biophysics, University of Washington, Seattle, WA 98195, USA

[2] BRIGHT-UP Summer Research Program, University of Washington School of Medicine, Seattle, WA 98195, USA

[3] Department of Microbiology, Immunology, and Molecular Genetics, University of California, Los Angeles, Los Angeles, CA 90095, USA

[4] Molecular Biology Institute, University of California, Los Angeles, Los Angeles, CA 90095, USA

* corresponding author

Abstract (250-300 words)

Soil-transmitted parasitic nematodes infect over 1 billion people worldwide and are a common source of neglected disease. *Strongyloides stercoralis* is a potentially fatal skin-penetrating human parasite that is endemic to tropical and subtropical regions around the world. The complex life cycle of *Strongyloides* species is unique among human-parasitic nematodes in that it includes a single free-living generation featuring soil-dwelling, bacterivorous adults whose progeny all develop into infective larvae. The sensory behaviors that enable free-living *Strongyloides* adults to navigate and survive soil environments are unknown. *S. stercoralis* infective larvae display parasite-specific sensory-driven behaviors, including robust attraction to mammalian body heat. In contrast, the free-living model nematode *Caenorhabditis elegans* displays thermosensory behaviors that guide adult worms to stay within a physiologically permissive range of environmental temperatures. Do *S. stercoralis* and *C. elegans* free-living adults, which experience similar environmental stressors, display common thermal preferences? Here, we characterize the thermosensory behaviors of the free-living adults of *S. stercoralis* as well as those of the closely related rat parasite, *Strongyloides ratti*. We find that *Strongyloides* free-living adults are exclusively attracted to near-tropical temperatures, despite their inability to infect mammalian hosts. We further show that lifespan is shorter at higher temperatures for free-living *Strongyloides* adults, similar to the effect of temperature on *C. elegans* lifespan. However, we also find that the reproductive potential of the free-living life stage is enhanced at warmer temperatures, particularly for *S. stercoralis*. Together, our results reveal a novel role for thermotaxis to maximize the infectious capacity of obligate parasites and provide insight into the biological adaptations that may contribute to their endemicity in tropical climates.

Author Summary (150-200 words)

Soil-transmitted parasitic nematodes infect over 1 billion people and are a major source of neglected disease, particularly in the world's most resource-limited communities. For most parasitic nematode species, reproductive adults exclusively reside within host animals. Species in the genus *Strongyloides* have a unique step in their life cycle that features soil-dwelling, non-parasitic adults. Previous studies of the free-living model nematode *Caenorhabditis elegans* have identified temperature as an important factor in ability of free-living nematodes to survive and reproduce in the environment. Our study investigates how the thermosensory behaviors of *Strongyloides* free-living adults contribute to their survival as well as their role in amplifying the quantity of infective larvae in the soil. We show that *Strongyloides* free-living adults display broad thermophilic preferences that are highly distinct from those of *C. elegans* adults. We also present the first evidence that thermotaxis acts as a robust mechanism for maximizing the infectious capacity of *Strongyloides* species located in tropical climates.

57 **Introduction**

58 Soil-transmitted parasitic nematodes are estimated to infect over 1 billion people worldwide and
59 can cause a range of debilitating symptoms, including chronic gastrointestinal distress, anemia,
60 malnutrition, and impaired growth in children [1–3]. The skin-penetrating human parasite
61 *Strongyloides stercoralis* is estimated to infect at least 600 million people [4–7]. Chronic
62 *S. stercoralis* infections, which arise due to the unique capacity of *S. stercoralis* to autoinfect
63 hosts, can go undetected for many decades before evolving into a life-threatening systemic
64 hyperinfection if an individual becomes immunocompromised [2,8,9]. Soil-transmitted parasitic
65 worms primarily affect impoverished communities and places that lack adequate sewage
66 management [6,7,10,11]. Current treatments only target ongoing infections and can be
67 inadequate; no medical treatment exists to prevent infection or reinfection [12–14]. Additionally,
68 there are currently a limited number of anthelminthic drugs, and anthelminthic resistance is
69 already widespread among livestock parasites due to repeated dosage with anthelminthic drugs
70 as part of regular deworming schedules [15,16]. Identifying novel therapeutic strategies, before
71 drug resistance develops in humans, is therefore an important global health priority.

72

73 Many soil-transmitted parasitic nematodes have a life cycle that starts with developmentally
74 arrested third-stage infective larvae (iL3s) finding and infiltrating a host animal [17]. Once inside
75 a host, iL3s resume development and migrate through various host tissues to the small intestine,
76 where they take up residence as parasitic adults. Parasitic adults produce offspring that are then
77 voided from the host in feces. These offspring develop into iL3s and restart the cycle. Species
78 in the genus *Strongyloides* have an additional, unique step in their life cycle, in which a fraction
79 of the offspring of parasitic adults can alternatively develop into morphologically distinct free-
80 living adults instead of infective larvae (Fig. S1) [8,18,19]. The offspring of these free-living adults

81 exclusively develop into iL3s that then must find and invade host animals. The molecular
82 mechanisms that drive the choice between homogonic development (post-parasitic larvae
83 become iL3s) and heterogonic development (post-parasitic larvae become free-living adults) is
84 poorly understood; however, the developmental decision depends on species identity, strain
85 genetics, host immunocompetency, and environmental temperatures [20–25]. For example,
86 exposure to temperatures above 34°C promotes direct development into iL3s for *S. stercoralis*,
87 presumably to allow larvae to develop into iL3s while still inside the host; these iL3s re-penetrate
88 host tissues to establish an autoinfection [2,9,21]. The free-living generation of *Strongyloides*
89 spp. allows these species to sexually reproduce; unlike hookworms, *Strongyloides* parasitic
90 adults are all genetically female and produce clonal progeny via parthenogenesis [8,20,26–29].
91 Furthermore, the *Strongyloides* free-living generation has been proposed to act as a means of
92 amplifying the number of infective larvae that a single parasitic female can produce [30]. Despite
93 its role in the *Strongyloides* life cycle, the *Strongyloides* free-living generation is generally
94 understudied [31]. A better understanding of the sensory physiology and behavioral repertoires
95 displayed by free-living *Strongyloides* adults could enable the development of novel strategies
96 for predicting and controlling the infectious capacity of a neglected source of human disease.
97
98 The free-living adults of *Strongyloides* spp. live in the soil and experience similar environmental
99 stressors to *Caenorhabditis elegans*, a nematode that is free-living throughout its entire life cycle.
100 Furthermore, *Strongyloides* free-living adults share many morphological similarities with
101 *C. elegans* adults [30,32,33]. Thus, to understand how sensory behaviors enable *Strongyloides*
102 free-living adults to survive in the environment, we can compare their behaviors to those of
103 *C. elegans*. One of the most ethologically significant and well-documented sensory behaviors
104 exhibited by *C. elegans* is thermosensory navigation. *C. elegans* uses a complex set of

105 thermosensory behaviors to stay within a physiologically and reproductively permissible
106 temperature range (15-25°C) [34–41]. In brief, *C. elegans* will utilize both positive and negative
107 thermotaxis to migrate towards a "remembered" cultivation temperature; at its cultivation
108 temperature, *C. elegans* will engage in isothermal tracking [35,38]. At noxious temperatures
109 ≥27°C and ≤5°C, *C. elegans* engage in noxious temperature responses, including reorientation
110 behaviors and accelerated migration towards physiological temperatures [40,42]. These
111 behavioral strategies are a critical mechanism for thermoregulation by a non-parasitic ectotherm:
112 exposure to noxious heat stress causes dramatic drops in *C. elegans* fertility and longevity, in a
113 manner partially dependent on strain and experience [34,43–50].
114
115 In comparison to *C. elegans*, the sensory behaviors and physiological requirements of soil-
116 transmitted parasitic nematodes are far less documented. The few studies that have quantified
117 the sensory behaviors of parasitic nematodes have demonstrated that the worms can detect a
118 range of sensory cues, including chemosensory and thermosensory stimuli [51–54]. For
119 thermosensation, recent work has shown that the iL3s of multiple mammalian-parasitic
120 nematode species, including *S. stercoralis*, display highly robust parasite-specific
121 thermosensory behaviors [55,56]. These include positive thermotaxis towards mammalian body
122 heat and negative thermotaxis towards below-ambient temperatures; the switch between these
123 two behavioral regimes is dictated by the ambient cultivation temperature, such that worms
124 exposed to temperatures above ambient will engage in positive thermotaxis (and vice versa)
125 [55]. As opposed to thermosensory behaviors being primarily used for physiological
126 thermoregulation (as with *C. elegans*), the positive thermotaxis behaviors of iL3s are thought to
127 reflect active host seeking; negative thermotaxis behaviors are potentially a mechanism enabling
128 iL3s to either disperse from host feces or disengage from accidental heat seeking towards a

129 non-host heat source [55,56]. Chemosensory behaviors also contribute to host-seeking and
130 host-invasion behaviors by soil-transmitted parasites [52,53,57]. Indeed, life-stage-specific
131 chemosensory preferences have previously been proposed to contribute to the restriction of
132 host-seeking behaviors to iL3s. For example, although *Strongyloides* iL3s and free-living adults
133 are both attracted to a variety of host odorants, only free-living larvae and adults are attracted to
134 fecal odors [53,57]. These findings suggest that downregulation of attraction to fecal odors
135 enables iL3s to disperse from feces in search of hosts [53,57]. Finally, although the impact of
136 multisensory cues on parasite behavior has not been thoroughly investigated, initial work has
137 indicated a sensory hierarchy in which strong thermal drive can override attraction to host-
138 associated odorants in iL3s [55]. Importantly, this hierarchy depends on the specific thermal
139 context in which an odorant is located. At temperatures below human skin temperature (~34°C),
140 the infective larvae appear to ignore attractive odorants in favor of warmer temperatures [55]. In
141 contrast, if an odorant is placed at temperatures closer to ~34°C, the infective larvae will
142 decrease thermotaxis behaviors and increase local search behaviors [55]. Together, these
143 findings suggest a sensory-dependent host-seeking strategy in which soil-transmitted iL3s first
144 navigate towards a heat source, then determine whether that heat source is a potential host.
145
146 The thermosensory preferences of *Strongyloides* free-living adults are completely unknown. Do
147 the physiological and behavioral responses of *Strongyloides* free-living adults to different
148 environmental temperatures mirror those exhibited by *C. elegans* adults? To answer this
149 question, we conducted a quantitative analysis of the thermal preferences and physiology of the
150 free-living adults of two *Strongyloides* species: the human parasite *S. stercoralis* and the closely
151 related rodent parasite *Strongyloides ratti.* We found that the thermosensory behaviors of
152 *Strongyloides* free-living adults are distinct from both *Strongyloides* infective larvae and

153 *C. elegans*. Across a broad range of thermal gradients, including those that trigger negative
154 thermotaxis in iL3s and noxious heat escape in *C. elegans*, *Strongyloides* free-living adults
155 display thermophilic migration. In addition, *S. stercoralis* free-living adults show a shifted
156 multisensory hierarchy, such that chemosensory attractants influence behavior at temperatures
157 below mammalian body heat. Finally, we discover that although attraction to warm temperatures
158 shortens the lifespan of *S. stercoralis* free-living adults, their reproductive potential is enhanced.
159 Our results suggest that *Strongyloides* free-living adults, whose progeny exclusively develop into
160 infective larvae, use thermotaxis navigation as a mechanism to enhance the number of infective
161 larvae in the soil. Together, these findings reveal biological adaptations that likely enhance the
162 transmission of a potentially fatal human-parasitic nematode in tropical and subtropical climates.
163

164 **METHODS**

165

166 All protocols and procedures involving vertebrate animals were approved by the UCLA Office of
167 Animal Research Oversight (Protocol ARC-2011-060) and by the UW Office of Animal Welfare
168 (Protocol 4570-01), which adhere to the standards of the AAALAC and the *Guide for the Care*
169 *and Use of Laboratory Animals*.
170

171 **Maintenance of *Strongyloides stercoralis***

172 *S. stercoralis* UPD strain was serially passaged through male Mongolian gerbils (Charles River
173 Laboratories) and maintained on fecal-charcoal plates as previously described [18]. Gerbils were
174 inoculated with ~2,250 iL3s in 200 μL sterile phosphate buffered saline (PBS) via inguinal
175 subcutaneous injection, under isoflurane anesthesia. Feces containing *S. stercoralis* were
176 collected by placing infected gerbils on wire-bottomed cages overnight, with damp Techboard

177 liners (Shepard Specialty Papers) on the cage bottoms. Fecal pellets were collected in the
178 morning, mixed with autoclaved charcoal granules (Ebonex), and stored in 10-cm-diameter Petri
179 dishes lined with Whatman filter paper. Fecal charcoal plates were stored at either 20°C for 48
180 hours or 25°C for 24 hours, then used in behavioral assays (free-living adults) or transferred to
181 23°C for 5-14 days until use (iL3s). *S. stercoralis* free-living adults and iL3s were collected from
182 fecal-charcoal plates using a Baermann apparatus, as previously described [58]. For brood size,
183 survival, and hatching assays, free-living adults were briefly suspended in BU worm saline [59]
184 in a watch glass; individual worms were then pipetted onto assay plates using a dissecting
185 microscope (Leica S9E).
186
187 **Maintenance of *Strongyloides ratti***
188 *S. ratti* ED321 strain was serially passaged through female Sprague Dawley rats (Envigo) and
189 maintained on fecal-charcoal plates as for *S. stercoralis*. Rats were inoculated with ~700 iL3s in
190 200 µL sterile PBS via inguinal subcutaneous injection, under isoflurane anesthesia. Collection
191 and storage of feces containing *S. ratti* was performed as described for *S. stercoralis*.
192
193 **Maintenance of *C. elegans***
194 *C. elegans* N2 strain (*Caenorhabditis* Genome Center, CGC) was maintained using standard
195 methods [60]. In brief, young adult hermaphrodites used for maintenance and thermotaxis
196 assays were raised on 2% Nematode Growth Media (NGM) plates seeded with a lawn of
197 *Escherichia coli* OP50 bacteria (CGC; maintenance plates). To generate age-synchronized
198 young adults for behavioral assays, adult hermaphrodites were allowed to lay eggs on
199 maintenance plates for 4 hours; adults were then removed, and the plates were stored at either
200 20°C or 23°C until progeny reached the desired life stage.

201

202 **Thermotaxis assays**

203 Thermotaxis assays were performed on a custom thermoelectric behavioral arena, as previously
204 described [49]. For some experiments, the thermoelectric control circuit included updated
205 electrical components; a full parts list and wiring diagram are archived in a dedicated GitHub
206 repository (https://github.com/BryantLabUW/Strongyloides-Free-Living-Thermosensory-
207 Behaviors). Worm migrations were visualized using a 20 MP CMOS camera (Basler Ace
208 acA5472-17um, Basler) at a frame rate of 0.2 frames per second for 45 minutes (adults) or 0.5
209 frames per second for 15 minutes (iL3s) using the pylon Viewer camera software suite (v7.4.0,
210 Basler). Thermotaxis experiments were carried out on age-synchronized young adult
211 hermaphrodites (*C. elegans*) and free-living adult males and females (*S. stercoralis*, *S. ratti*) that
212 were incubated for at least 2 hours at the desired cultivation temperature (15°C, 20°C, or 23°C).
213 For iL3 assays, worms were collected with a Baermann apparatus and suspended in ~1 mL BU
214 saline in a watch glass, then incubated for at least 2 hours at the appropriate temperature. For
215 multisensory assays, 5 µL of undiluted 3-methyl-1-butanol was placed on the thermotaxis plate
216 immediately before worms were deposited. For *post-hoc* measurements of individual worm
217 movements, x/y coordinates were generated using the Manual Tracking plugin for Fiji, then
218 quantified and plotted using custom MATLAB scripts (MathWorks), as previously described
219 [55,56,61]. All custom code and hardware specifications are archived on GitHub
220 (https://github.com/BryantLabUW/Strongyloides-Free-Living-Thermosensory-Behaviors).

221

222 **Brood size and survival assays**

223 For *C. elegans*, age-synchronized adult hermaphrodites with 1-5 eggs were picked from
224 maintenance plates onto treatment plates (2% NGM plates seeded with 50 µL HB101 bacteria)

225 and allowed to grow for 1-3 days. For *S. stercoralis* and *S. ratti*, free-living adult females with
226 fewer than five eggs and 3 free-living males were pipetted from a BU-filled watch glass onto
227 treatment plates. Plates were randomly divided among the treatment temperatures (23°C, 30°C,
228 or 37°C) and moved to their respective incubators. Experiments were performed in batches of
229 at least two temperature conditions. Worms were checked for survival (movement or pharyngeal
230 pumping) and brood size (number of eggs and larvae on plate) every 24 hours. If the worm was
231 still alive, it was moved to a new treatment plate and returned to its treatment incubator for
232 another 24 hours. This process was repeated until all worms had died. On the day each worm
233 died, the number of eggs/larvae present when each plate was checked was recorded.
234

235 **Hatching viability assays**

236 Age-synchronized adult hermaphrodites (*C. elegans*) and free-living adult females
237 (*S. stercoralis*, *S. ratti*) with greater than five eggs were transferred from maintenance plates
238 (*C. elegans*) or a BU-filled watch glass (*S. stercoralis*, *S. ratti*) onto treatment plates. All
239 treatment plates were moved to a 23°C incubator for four hours to allow worms to lay eggs. After
240 four hours, adult worms were removed, and the number of eggs laid on each plate was recorded
241 (E_0). Plates with fewer than eight eggs were excluded from the experiment. Plates were
242 randomly divided among the treatment temperatures (23°C, 30°C, or 37°C) and moved to their
243 respective incubators. Experiments were done in batches of at least two temperatures at a time.
244 After 24 hours, the number of eggs remaining on treatment plates was recorded (E_1). Hatching
245 viability was then calculated using the following formula:

246 $$(E_0 - E_1)/E_0 * 100$$

247

248 **Statistical analysis**

249 All statistical analyses except mean survival were conducted using GraphPad Prism 10
250 (Dotmatics). Mean survival values were calculate using OASIS 2 [62] Power analyses to
251 determine appropriate sample sizes were performed using G*Power 3.1 [63]. Statistical details
252 for experiments are provided in figure legends and Supplemental Data File 1.
253

254 **Results**

255 **The free-living adults of *Strongyloides* species prefer temperatures warmer than their**
256 **cultivation temperature.**

257 To begin characterizing the temperature preferences of *Strongyloides* free-living adults, we first
258 looked to see if they display behaviors similar to those of the constitutively free-living model
259 nematode *C. elegans*. One well-documented behavior of *C. elegans* is that well-fed adult
260 hermaphrodites migrate towards a remembered cultivation temperature when placed on a
261 thermal gradient within their physiological temperature range (15-25°C) [34–36,39,40]. To test if
262 *Strongyloides* free-living adults display similar thermal preferences, we generated post-parasitic
263 free-living adults by cultivating feces containing post-parasitic larvae at 20°C for two days. Next,
264 we placed isolated free-living females (FLFs) at 23°C in a large-format thermotaxis arena in
265 which we established a ~21-25°C temperature gradient. Under these conditions, *C. elegans*
266 adult hermaphrodites that were raised at 20°C displayed negative thermotaxis towards their
267 cultivation temperature, as expected (Fig. 1 A, D). In contrast, we observed that *S. stercoralis*
268 FLFs were more likely to engage in positive thermotaxis (Fig. 1B, D, E). *S. ratti* free-living
269 females also did not migrate towards their cultivation temperature, instead displaying attraction
270 to above-ambient temperatures, similar to *S. stercoralis* (Fig. 1C-E). We also tested the thermal
271 preferences of *Strongyloides* free-living males (FLMs). *S. stercoralis* FLFs and FLMs displayed
272 similar behaviors, while *S. ratti* FLFs traveled slightly further up the gradient than *S. ratti* FLMs

273 (Fig. S2). The difference between *S. ratti* FLFs and FLMs was not due to systemic differences
274 in velocity, as we observed no significant difference in mean speed (mm/s) between sexes (Fig.
275 S2C).
276
277 ***S. stercoralis* free-living females show positive thermotaxis in conditions that elicit**
278 **noxious temperature escape behavior in *C. elegans* adults.**
279 Another critical aspect of the *C. elegans* free-living thermosensory repertoire is the avoidance of
280 noxious temperatures [37,64–66]. Experimentally, escape from noxious heat can be observed
281 by placing adult hermaphrodites above 26°C, triggering migration down the thermal gradient
282 towards physiologically permissive temperatures [37,38,40]. Notably, the behavioral strategies
283 and cellular mechanisms underlying noxious temperature responses are partially distinct from
284 those driving innocuous temperature responses [37,50,66–68]. To determine if thermal escape
285 behaviors are present in *Strongyloides* FLFs, we compared the migration of *C. elegans* adult
286 hermaphrodites and *Strongyloides* FLFs placed at 30°C in a ~21-35°C gradient (cultivation
287 temperature, T_C = 23°C). As expected, *C. elegans* hermaphrodites showed robust migration
288 towards cooler temperatures (Fig. 2A, D, E). Surprisingly, neither *Strongyloides* species
289 displayed noxious temperature avoidance behaviors (Fig. 2B-E). *S. stercoralis* FLFs continued
290 to show positive thermotaxis towards 34°C (Fig. 2B). In contrast, *S. ratti* FLFs did not significantly
291 disperse from their starting temperature of 30°C (Fig. 2C-E). Finally, we tested whether
292 *S. stercoralis* FLFs would display noxious temperature responses when exposed to mammalian
293 core body temperatures. We found that *S. stercoralis* FLFs placed at 37°C in a ~32-38°C
294 gradient did not migrate down the gradient (T_C = 23°C; Fig. S3). Together, these results indicate
295 that the thermal preferences of *Strongyloides* free-living adults are distinct from those of
296 *C. elegans* adult hermaphrodites, despite the similarities in their ecological niches (*i.e.*, they are

297 both non-parasitic bacterivores). Furthermore, it suggests that the cellular mechanisms that
298 produce robust behavioral responses to noxious heat in *C. elegans* are either not present in
299 *Strongyloides* spp., are tuned for temperatures much higher than mammalian body heat or have
300 been co-opted for other functions.
301
302 **Free-living adults display thermal preferences that are distinct from iL3s.**
303 The iL3s of multiple mammalian-parasitic nematode species, including *S. stercoralis* and *S. ratti,*
304 engage in negative thermotaxis towards cooler temperatures when placed near or below their
305 ambient cultivation temperature [55,56]. This preference for cooler temperatures may act as a
306 mechanism to disperse iL3s into cooler soil environments where discrimination between host-
307 emitted heat and environmental temperatures is maximized. What are the behaviors of
308 *Strongyloides* FLFs in cooler gradients? We first tested the preferences of *S. stercoralis* FLFs in
309 a ~12-22°C gradient, conditions in which *S. stercoralis* iL3s engage in negative thermotaxis and
310 accumulate at ~16°C (Fig. S5) [56]. Surprisingly, we found that *S. stercoralis* FLFs displayed
311 relatively robust positive thermotaxis in these conditions (Fig. S5B, F). To test whether *S. ratti*
312 display similar life-stage-specific differences in negative thermotaxis, we first tested the
313 preferences of *S. ratti* iL3s in the ~12-22°C gradient. We found that *S. ratti* iL3s stayed closer to
314 their starting temperature than *S. stercoralis* iL3s (Fig. S5C, E). Nevertheless, *S. ratti* FLFs also
315 engaged in positive thermotaxis when placed at 20°C (Fig. SD, F). Together with our earlier
316 experiments at above-ambient temperatures, these results indicate that *Strongyloides* FLFs are
317 biased towards performing positive thermotaxis across a broad range of environmental
318 temperatures.
319

320 ***Strongyloides* spp. FLFs respond to host-associated odorants in near-ambient**
321 **temperature gradients.**
322 Like *C. elegans*, *Strongyloides* spp. can detect a range of non-thermosensory stimuli, including
323 chemosensory cues [51,53,57,69]. In near-ambient temperature gradients, *S. stercoralis* iL3s
324 prioritize thermosensory behaviors over chemosensory responses, such that exposure to
325 temperature gradients below host body heat can override attraction to a host-associated odorant
326 [49]. Do *S. stercoralis* FLFs display a similar sensory hierarchy? To test this question, we
327 evaluated the impact of the attractive odorant 3-methyl-1-butanol (3m1b) on the behavior of
328 *S. stercoralis* FLFs in a ~20-25°C gradient. In the absence of an odorant, *S. stercoralis* FLFs
329 placed at 23°C displayed positive thermotaxis, traveling towards warmer temperatures (Fig. 1B-
330 E; Fig. 3). In the presence of an odorant placed either near to the starting position of the worms
331 (odorant location: 22.5°C, ~2.7 cm from T_{start}), or further away (odorant location: 22°C, ~5.5 cm
332 from T_{start}), we observed a decrease in the distance individual worms traveled up the gradient
333 when compared to worms in a pure thermotaxis (*i.e.*, no odorant) gradient (Fig. 3; Fig. S6). The
334 reduction partially reflects an increase in the number of worms that initially traveled down the
335 temperature gradient towards the odorant before traveling back up the gradient (Fig. S6). This
336 shifted migratory pattern was particularly noticeable when the odorant was placed in the "far"
337 location (Fig. 3C; Fig. S6B). These results suggest a difference in the sensory hierarchy
338 underlying the behaviors of *S. stercoralis* FLFs and iL3s, such that the FLF sensory hierarchy is
339 less dominated by temperature cues (Fig. 4).
340
341 **Increasing cultivation temperature decreases the lifespan of *Strongyloides* FLFs.**
342 The multifaceted repertoire of thermosensory behaviors exhibited by *C. elegans* free-living
343 adults (*i.e.*, experience-dependent migration towards ambient cultivation temperature,

344 isothermal tracking of cultivation temperature, and robust avoidance behaviors associated with
345 noxious temperatures) are thought to be methods of thermoregulation in support of survival and
346 reproduction [34–38,40,67,68]. Thus, our observation that the free-living adults of *Strongyloides*
347 species almost exclusively engage in migration to above-ambient temperatures is highly
348 intriguing. To begin searching for an explanation for the thermophilic preferences of
349 *Strongyloides* free-living adults, we tested the impact of different constant environmental
350 temperatures on the survival of free-living females (Fig. 5, Fig. S7). Individual *S. stercoralis* and
351 *S. ratti* FLFs, as well as *C. elegans* hermaphrodites, were placed on NGM plates seeded with
352 *E. coli* HB101 at either 23°C, 30°C, or 37°C and their survival was checked daily (Fig. 5A). As
353 expected, increasing the cultivation temperature of *C. elegans* adults resulted in a dramatic
354 decrease in lifespan (Fig. 5B, E). When the cultivation temperature was increased for
355 *S. stercoralis* and *S. ratti* FLFs, the lifespan of both *Strongyloides* species also decreased (Fig.
356 5C, D, E). Notably, this decreased survival at warmer temperatures appears to conflict with the
357 thermal preferences of the free-living adults. This raises the question of why *Strongyloides* FLFs
358 are attracted to temperatures that decrease their longevity.
359

360 ***S. stercoralis* FLFs show increased reproductive success at near-tropical temperatures**

361 One possibility is that the thermal preferences of *Strongyloides* FLFs support other critical
362 biological processes – in particular, the reproductive capacity of this life stage. To test the
363 hypothesis that exposure to warmer temperatures positively impacts *Strongyloides* reproduction,
364 we counted the number of offspring produced by individual FLFs cultivated at different
365 temperatures (Fig. 6A). Similar to previous studies, we found that exposure to warm
366 temperatures rapidly and dramatically depresses *C. elegans* total brood size (Fig. 6B, Fig. S8)
367 [45,46]. In contrast, *S. stercoralis* FLFs showed a significant increase in total brood size at 30°C

368 (Fig. 6B). When the temperature was increased further to 37°C, we observed a decrease in total
369 brood size such that the total numbers of eggs and larvae produced at 23°C and 37°C are not
370 statistically different (Fig. 6B). This decrease in total brood size primarily reflects the decreased
371 lifespan of *S. stercoralis* FLFs at 37°C. When we examined the number of eggs and larvae laid
372 each day, we observed an increase in *S. stercoralis* daily brood size at 37°C compared to 23°C
373 on the first experimental day (Fig. S8). Thus, the mechanisms that yield enhanced total brood
374 sizes at 30°C are likely also active at 37°C; however, those increases are offset by decreased
375 longevity of the FLFs. We also tested the impact of warm temperatures on *S. ratti* total brood
376 sizes and found that they exhibited no change in total brood size between 23°C and 30°C and a
377 decreased total brood size at 37°C (Fig. 6B). When we compared the *S. ratti* day-by-day brood
378 sizes, we observed that exposure to 30°C did drive an initial increase in daily brood size
379 compared to 23°C, similar to *S. stercoralis* (Fig. S8). These results suggest that *S. stercoralis* is
380 physiologically adapted for warmer climates than *S. ratti*, which mirrors the geographical
381 distributions of these two species: *S. ratti* is widely distributed throughout the world while
382 *S. stercoralis* is most prevalent in tropical and subtropical climates [10,11,70].
383
384 In *C. elegans*, exposure to noxious warmth not only decreases brood size but also decreases
385 hatching viability [48,49,71,72]. The effect of increased temperature on *Strongyloides* FLF's egg
386 hatching viability is unknown and is particularly interesting because of our finding that
387 *Strongyloides* brood sizes can be enhanced at warmer temperatures. Increased brood sizes
388 could reflect compensatory mechanisms if the hatching viability of *Strongyloides* spp. is
389 decreased at warmer temperatures, similar to *C. elegans*. Alternatively, hatching viabilities that
390 are largely unaffected by warmer temperatures could indicate that parasites are generally
391 adapted to warmer environmental temperatures. To determine hatching viability, we collected

392 synchronized eggs by letting individual *C. elegans* adult hermaphrodites and *Strongyloides* adult
393 FLFs lay eggs onto NGM plates seeded with *E. coli* HB101 for 4 hours at 23°C. After removing
394 the adults, we counted the number of eggs on each plate, then incubated plates at either 23°C,
395 30°C, or 37°C for 24 hours (*C. elegans*) or 48 hours (*Strongyloides* spp.) before re-counting any
396 unhatched eggs (Fig. 6C). As expected, we observed that *C. elegans* median hatching viability
397 progressively decreased as a function of increased temperature (Fig. 6D). In contrast,
398 *S. stercoralis* did not show any significant change in hatching viability as cultivation temperature
399 increased up to 37°C (Fig. 6D). *S. ratti* also exhibited no significant change in hatching viability
400 from 23°C to 30°C; however, we did observe a small, but significant, decrease in hatching
401 viability when cultivated at 37°C (Fig. 6D). Notably, this decreased *S. ratti* hatching viability was
402 still significantly higher than the *C. elegans* hatching viability at 37°C ($p<0.0001$, 2-way ANOVA
403 with Tukey's multiple comparisons test). Together, these experiments indicate that the range of
404 reproductively and developmentally permissive temperatures is shifted towards warmer
405 temperatures for *Strongyloides* spp. compared to *C. elegans*.
406

407 **Discussion**

408 Here, we present the first characterization of thermosensory behaviors by *Strongyloides* free-
409 living adults and provide evidence to link life-stage-specific thermal preferences to physiological
410 and reproductive consequences. We found that the free-living adults of *S. stercoralis* are
411 attracted to above-ambient temperatures in a wide range of thermal conditions, including
412 temperature gradients that trigger noxious heat escape behaviors in *C. elegans*, negative
413 thermotaxis towards cultivation temperature in *C. elegans*, and negative thermotaxis towards
414 below-ambient temperatures in *S. stercoralis* iL3s (Fig. 7). We showed that unlike iL3s,
415 *S. stercoralis* free-living females can respond to chemosensory attractants in thermal gradients

416 below human body temperature. Impressively, we saw that some worms can even migrate
417 against their thermal preferences in favor of moving towards the odorant. We also performed the
418 first systematic evaluation of the impact of environmental temperatures on the physiological and
419 reproductive potential of *S. stercoralis* free-living adults. We found that exposure to 30°C drives
420 an unexpected increase in the brood size of *S. stercoralis* free-living adults, even at the expense
421 of their longevity. Finally, comparisons between *S. stercoralis* and *S. ratti* reveal that *S.*
422 *stercoralis* is adapted to warmer temperatures than *S. ratti*, a difference that aligns with their
423 narrower geographic distribution [10,11,70].
424
425 Free-living nematodes can experience a range of environmental stressors; as ectotherms,
426 environmental temperature is a critical source of potential stress that can significantly impact
427 their individual fitness. The free-living model nematode *C. elegans* displays a complex
428 thermoregulatory process that, in response to thermal stress, prioritizes individual survival and
429 future fecundity over immediate production of offspring [73,74]. Major elements of the *C. elegans*
430 thermoregulatory response include thermotaxis navigation towards physiologically permissive
431 temperatures, inhibition of reproduction, and altering a range of other physiological processes
432 [34,43,45,48,73,74]. Until now, it has been unclear whether this thermoregulatory strategy was
433 a ubiquitous feature of ectothermic, bacterivorous nematodes. Our results demonstrate that the
434 free-living adults of two nematode species, *S. stercoralis* and *S. ratti*, display an alternative
435 thermoregulatory strategy, one that prioritizes immediate expansion of infective larval
436 populations over individual adult survival. These findings demonstrate that despite their
437 similarities to *C. elegans*, *Strongyloides* free-living adults display distinct thermosensory
438 responses and physiological characteristics, underscoring the potential for diversity in the
439 behaviors of ectotherms inhabiting ostensibly similar ecological niches.

440

441 Previous studies have found large differences in thermal preferences between *C. elegans* adults
442 and host-seeking *Strongyloides* iL3s [55,56]. Our current results expand these differences to
443 *Strongyloides* free-living adults. The specialized thermotaxis behaviors of *S. stercoralis* iL3s are
444 thought to arise from adaptations to a neural circuit that is conserved with *C. elegans*. Our
445 findings suggest that these adaptations are a persistent feature of the *Strongyloides*
446 thermosensory circuit across life stages. However, our data also reveals plasticity in the
447 thermosensory behaviors of *Strongyloides* as a function of life stage, specifically, the failure of
448 *Strongyloides* FLFs to perform negative thermotaxis, a behavior that is robustly present in
449 *Strongyloides* iL3s. These differences mirror the life-stage-specific differences in chemosensory
450 preferences previously observed with *Strongyloides* species [52,53,57]. In *C. elegans*, changes
451 in the behavioral valence of sensory stimuli across life stages can arise from plasticity in the
452 functional architecture of sensory neural microcircuits [67,75,76]. Similar life-stage-specific
453 changes in functional connectivity could account for the behavioral differences we see between
454 *Strongyloides* iL3s and free-living adults. Taken together, our results emphasize the need for
455 future studies that pinpoint the neural mechanisms that drive parasite-specific and life-stage-
456 specific thermotaxis behaviors in *Strongyloides* species.

457

458 Our experiments demonstrate that soil-resident *Strongyloides* free-living adults cannot survive
459 prolonged exposure to temperatures approximating mammalian body heat. This physiological
460 inability contrasts strongly with the ability of host-resident *Strongyloides* parasitic adults to
461 survive for many months within host bodies, as well as the ability of soil-resident iL3s to survive
462 the thermal transition associated with host invasion [77]. Thus, ectothermic species that
463 parasitize warm-blooded animals are not innately resistant to the negative impacts of thermal

464 stress. What are the molecular and cellular mechanisms that not only enable *Strongyloides*
465 parasitic adults to survive and reproduce within the host environment, but also produce a
466 remarkable increase in maximum lifespan compared to free-living adults [30,77,78]? If these
467 mechanisms are actively acquired or maintained following host infection, they may represent an
468 exciting source of molecular targets for novel anthelmintic drugs. In the future, we hope that
469 research leveraging our mechanistic understanding of *C. elegans* thermal physiology and the
470 growing *Strongyloides* genetic toolkit will provide insight into the remarkable physiological
471 abilities of parasitic adults [69,79].
472
473 Here, we have focused on understanding the thermotaxis behaviors and thermal physiology of
474 *Strongyloides* free-living adults, a life stage observed only in *Strongyloides* and the closely
475 related *Parastrongyloides* genera [80]. Although other medically important parasitic species,
476 such as human hookworms, lack a free-living generation, they do deposit eggs and larvae into
477 the environment that must also survive environmental temperatures long enough to mature into
478 infective larvae that will locate and infect host animals. Is the ability of *Strongyloides* post-
479 parasitic eggs to maintain high hatching viability in warm temperatures a common feature of
480 parasitic nematodes that are endemic to tropical and sub-tropical regions? Recent experimental
481 evidence is limited and potentially determined by experimental conditions: whereas one study
482 reports that the eggs of *Necator americanus*, a human hookworm, display low rates of hatching
483 at temperatures above 35°C, another reports that the eggs of both *N. americanus* and the human
484 hookworm *Ancylostoma duodenale* are able to hatch (albeit with increasing mortality) at
485 temperatures up to 40°C [81,82]. The eggs of other parasitic nematode species, including the
486 pig large roundworm *Ascaris suum*, also display remarkable resistance to elevated temperatures
487 [83–87]. For behavioral preferences, previous studies have found that *S. stercoralis* iL3s prefer

488 temperatures warmer than the human hookworm *Ancylostoma ceylanicum* and other
489 mammalian-parasitic nematodes [55]. Thus, the ability of *S. stercoralis* FLFs to maintain high
490 hatching viability at 37°C may indicate a particularly high thermal tolerance, even among human-
491 parasitic nematodes. Nevertheless, mammalian parasites must all survive and reproduce at
492 body heat, suggesting the possibility of common molecular mechanisms for avoiding decreased
493 longevity and diminished fecundity due to heat stress.
494
495 Our investigation of the impact of environmental temperatures on the effective fecundity of the
496 *Strongyloides* free-living generation has intriguing implications for the role of this life stage in
497 promoting infections across diverse climates. Our experiments show that the reproductive
498 potential of *Strongyloides* free-living adults is relatively impervious to prolonged exposure to
499 30°C. Human infections with *S. stercoralis* predominantly occur in tropical and sub-tropical
500 climates [10,11]. Our results suggest that the specialized physiology of *S. stercoralis* can
501 contribute to the maintenance of infectious populations within these climates. Specifically, our
502 findings deepen our understanding of the complex relationship between temperature, the choice
503 between the heterogonic and homogonic developmental pathways, and the production of
504 infective larvae. Previous work has shown that *S. stercoralis* post-parasitic L1 larvae that
505 experience temperatures below 34°C are driven to develop into free-living adults [21]. Now, we
506 show that after reaching adulthood, *S. stercoralis* adults are attracted to warm temperatures,
507 potentially enhancing their reproductive output at the expense of individual longevity.
508 Furthermore, even in cases where total reproductive output is only maintained, rather than
509 enhanced (*e.g.*, *S. stercoralis* at 37°C), exposure to warmer temperatures will shorten the time
510 required to generate large numbers of iL3s, which may influence the functional infectivity of the
511 soil-dwelling population [88–90].

512

513 Together, our results suggest that the thermotaxis behaviors and thermal physiology of
514 *S. stercoralis* are particularly adapted for tropical climates. These findings are especially
515 concerning in the context of anthropogenic climate change, where increases in global
516 temperatures could shift the geographic ranges capable of supporting *S. stercoralis* transmission
517 while also improving reproductive capacity and functional infectivity of these parasites [91,92].
518 Ultimately, our work emphasizes the importance of developing a deeper understanding of the
519 complex behaviors and physiology of *S. stercoralis*, a highly neglected source of human disease.

520

521 **Acknowledgements**

522 We gratefully acknowledge Neil E. Warren and the University of Washington Instrumentation
523 Services. We thank Dr. Dana Miller and the Hot Buttered Mice group for their help regarding
524 survival assays and OASIS 2. We thank Yi Zhang, Kyle Thieringer, Rachel Oaks-Leaf, and Dr.
525 Dana Miller for insightful comments on the manuscript.

526

527 **Funding**

528 This work was supported by National Institutes of Health DP2AI184544 (A.S.B.), funds provided
529 by the University of Washington School of Medicine (A.S.B), National Institutes of Health
530 R01AI136976 (E.A.H), and funds provided by AstraZenica and an anonymous donor (J.S.).

531

532 **Figure Legends**

533

534 **Figure 1. Thermotaxis behaviors of *Strongyloides* free-living females near ambient**
535 **temperatures are distinct from those of *C. elegans* adults.**

536 For panels A-C, worms were placed at 23°C in a ~21-25°C gradient and allowed to migrate for
537 45 min. Cultivation temperature (T_C) = 20°C. Starting temperature (T_{start}) = 23°C (grey line). Black
538 crosses show the starting position of the worms. Representative tracks of *C. elegans* adult
539 hermaphrodites (A), *S. stercoralis* free-living females (FLFs) (B), and *S. ratti* FLFs (C). *C.*
540 *elegans* hermaphrodites are seen engaging in negative thermotaxis toward their cultivation
541 temperature, while *S. stercoralis* and *S. ratti* FLFs engage in positive thermotaxis.
542 D) Quantification of the change in temperature experienced by *C. elegans* adults, *S. stercoralis*
543 FLFs, and *S. ratti* FLFs. Values are the final temperature – starting temperature for each worm.
544 Icons indicate responses of individual worms, boxes show medians and interquartile ranges,
545 and whiskers show min and max values.
546 n = 54 worms for *C. elegans* hermaphrodites (5 assays across 4 days), n = 76 worms for
547 *S. stercoralis* free-living females (7 assays across 5 days), n = 59 worms for *S. ratti* FLFs (6
548 assays across 4 days). ns = not significant, ****p<0.0001, Kruskal-Wallis test with Dunn's
549 multiple comparisons test.
550 E) Categorical distribution of thermotaxis behaviors in a ~20-25°C gradient across species. For
551 each species, individual worms were considered to have engaged in positive or negative
552 thermotaxis if their position at the end of the assay was outside of a 1 cm neutral exclusion zone
553 centered on the starting position of each individual worm. Individuals that finished the assay
554 within this zone were considered non-responding. ***p<0.001, Fisher's exact test with
555 Bonferroni-Dunn correction for multiple comparisons.
556
557 **Figure 2. *Strongyloides* free-living females do not display noxious heat avoidance near**
558 **human skin temperature.**

559 Worms were placed at 30°C in a ~21-35°C gradient and allowed to migrate for 45 min. T_C =
560 23°C. Colored tracks represent the path of individual worms. Grey line represents T_{start} = 30°C.
561 Black crosses show the starting position of the worms. Representative tracks of *C. elegans* adult
562 hermaphrodites (A), *S. stercoralis* free-living females (B), and *S. ratti* free-living females (C).
563 *C. elegans* hermaphrodites are seen engaging in noxious heat escape behaviors while
564 *S. stercoralis* FLFs engage in positive thermotaxis and *S. ratti* FLFs engage in neither positive
565 nor negative thermotaxis.
566 D) Quantification of the change in temperature for *C. elegans* adults, *S. stercoralis* FLFs, and *S.*
567 *ratti* FLFs. Values are the final temperature – starting temperature for each worm. Icons indicate
568 responses of individual worms; boxes show medians and interquartile ranges; whiskers show
569 min and max values. n = 50 worms for *C. elegans* hermaphrodites (5 assays across 3 days), n
570 = 65 worms for *S. stercoralis* FLFs (5 assays across 3 days), n = 47 worms for *S. ratti* FLFs (6
571 assays across 4 days). ****p<0.0001, Kruskal-Wallis test with Dunn's multiple comparisons test.
572 E) Categorical distribution of thermotaxis behaviors in a ~21-35°C gradient across species.
573 Individuals were considered to have engaged in positive or negative thermotaxis if their position
574 at the end of the assay was outside of a 1 cm neutral exclusion zone centered on the starting
575 position of each individual worm. Individuals that finished the assay within this zone were
576 considered non-responding. ***p<0.001, Fisher's exact test with Bonferroni-Dunn correction for
577 multiple comparisons.
578
579 **Figure 3. *S. stercoralis* FLF's thermotaxis behavior is disrupted by the presence of an**
580 **attractive odorant.**
581 A) Diagram of the attractive odorant and temperature gradient experimental setup. Worms were
582 placed at 23°C in a ~21-25°C temperature gradient. An attractive odorant (3m1b) was either not

583 introduced, placed near the worm starting location (at 22.5°C), or placed far from the worm
584 starting location (at 22°C). Assay duration: 45 minutes. Temp only data is reproduced from Fig.
585 1.
586 B) Heat map showing the temperature experienced by individual worms throughout the 45-
587 minute assay. Cooler temperatures are represented by darker colors while warmer temperatures
588 are represented by warmer colors. Heatmap rows are ordered by hierarchical cluster analysis.
589 Triangles on the right of the heat maps indicate the individual worms chosen as representative
590 tracks in Fig. 3C.
591 C) Example tracks of individual worms from each experimental condition. Tracks are color coded
592 by time in the assay as seen in the scale on the right. Gray line = 23°C (T_{start}); black dots indicate
593 worm starting position.
594 D) Quantification of the change in temperature experienced by worms (final temperature –
595 starting temperature). Icons indicate responses of individual worms, boxes show medians and
596 interquartile ranges, and whiskers show min and max values. n = 76 worms for temperature only,
597 n = 65 worms for odorant near (6 assays over 3 days), and n = 66 worms for odorant far (6
598 assays over 3 days). ns = not significant, ***p*<0.01, ****p*<0.0001, Kruskal-Wallis test with Dunn's
599 multiple comparisons test.
600
601 **Figure 4. Comparison of the sensory hierarchy across *Strongyloides* life stages.**
602 Similar sensory cues result in different behaviors based on the sensory hierarchy of a specific
603 life stage (indicated by direction of scale icon). At near-ambient temperatures, iL3s prioritize
604 performing thermotaxis behaviors over responding to an attractive odorant [55]. At temperatures
605 near host body heat, iL3 migration is influenced by attractive host odorants [55]. In contrast, free-

606 living adults perform both thermotaxis and chemotaxis at near ambient temperatures, likely due
607 to a sensory hierarchy that is less dominated by temperature cues.
608
609 **Figure 5. Exposure to high temperatures decreases the lifespan of *Strongyloides* spp.**
610 **FLFs.**
611 A) Diagram of survival assay. Individual adults were placed on NGM plates seeded with *E. coli*
612 HB101. Individual worms were added to plates, then incubated at either 23°C, 30°C, or 37°C.
613 Plates were checked every 24 hours for survival. Black circles represent assays run at 23°C,
614 gold diamonds represent assays run at 30°C, and red triangles represent assays run at 37°C.
615 For all experiments, animals that were not found on the plate were censored. For *C. elegans*
616 and one *S. stercoralis* experiment, the dates of censoring were not recorded; these animals (3
617 for *C. elegans*, 2 for *S. ratti*) have been excluded from survival analyses. Number of censored
618 animals included in survival analyses = *C. elegans*: none; *S. stercoralis*: 5 (23°C), 0 (30°C), 0
619 (37°C); *S. ratti*: 4 (23°C), 5 (30°C), 6 (37°C). Survival curves reflect the combined survival of all
620 worms across 5 (*C. elegans*, *S. ratti*) or 6 (*S. stercoralis*) independent experiments for each
621 species. Survival curves for individual experiments are shown in Fig. S7.
622 B) Probability of survival over time for *C. elegans* adult hermaphrodites.
623 C) Probability of survival over time for *S. stercoralis* FLFs.
624 D) Probability of survival over time for *S. ratti* FLFs.
625 E) Table reporting average survival times for all species and temperature conditions. Values are
626 mean ± standard error (number of animals). *p*-values are pairwise comparison of survival curves
627 (23°C vs 30°C, 30°C vs 37°C, 23°C vs 37°C): $p<0.001$, Mantel-Cox test with Bonferroni-Dunn
628 correction for multiple comparisons.
629

630 **Figure 6. Impact of near-tropical temperatures on *S. stercoralis* FLF brood size.**

631 A) Diagram of the brood size assay. Individual adults were placed on NGM plates seeded with
632 *E. coli* HB101. Plates were incubated at either 23°C, 30°C, or 37°C and checked every 24 hours
633 for the number of eggs and larvae.

634 B) Quantification of the impact of environmental temperature on brood size for *C. elegans*
635 hermaphrodites (n = 36-47 adult worms), *S. stercoralis* free-living females (n = 32-54 adult
636 worms), and *S. ratti* free-living females (n = 29-38 adult worms). Icons indicate responses of
637 individual worms, boxes show medians and interquartile ranges, and whiskers show min and
638 max values. ns = not significant, ****p*<0.01, *****p*<0.0001, two-way ANOVA with Tukey's multiple
639 comparisons test.

640 C) Diagram of the hatching assay. Individual adults were placed on NGM plates seeded with
641 *E. coli* HB101. Plates were incubated for 4 hours at 20°C. After 4 hours, females were removed
642 from plates and eggs were counted. Plates were then incubated at 23°C, 30°C, or 37°C. After
643 24-48 hours, unhatched eggs were counted.

644 D) Quantification of hatching viability for *C. elegans* (n = 50-53 plates), *S. stercoralis* (n = 23-35
645 plates), and *S. ratti* (n = 22-27 plates). Icons indicate responses of individual worms, boxes show
646 medians and interquartile ranges, and whiskers show min and max values. ns = not significant,
647 ****p*<0.01, *****p*<0.0001, two-way ANOVA with Tukey's multiple comparisons test.

648

649 **Figure 7. Species- and life-stage-specific thermosensory behaviors and thermal**
650 **physiology**

651 A) Summary of *Strongyloides* iL3 thermotaxis behaviors. *Strongyloides* iL3s display two modes
652 of thermotaxis behavior: positive thermotaxis towards host body heat and negative thermotaxis
653 towards below-ambient temperatures [55,56]. If a temperature gradient ends below ~30°C,

654 *Strongyloides* iL3s are able to reverse an initial attraction to warmth, performing a "U-turn"
655 behavior that triggers sustained negative thermotaxis towards below-ambient temperatures [56].
656 B) Summary of *Strongyloides* FLF thermotaxis behaviors and physiological response to
657 increased temperatures. *Strongyloides* FLFs are attracted to temperatures above ambient.
658 Sustained exposure to above-ambient temperatures drives reductions in adult lifespan; in
659 contrast, brood size and hatching viability are enhanced (or stable) at near-tropical
660 temperatures.
661 C) Summary of *C. elegans* free-living hermaphrodite thermotaxis behaviors and physiological
662 response to increased temperatures. Between 15-25°C, *C. elegans* adults show attraction to a
663 "remembered" cultivation temperature and will undergo positive and negative thermotaxis
664 towards that temperature [34–36,39,40] . At temperatures greater than 26°C, *C. elegans* adults
665 display a noxious heat escape response and have a very decreased lifespan, brood size, and
666 hatching viability [34,37–39,42,43,50,64].
667
668 **Supplemental Information**
669 **Figure S1: Life cycles of *S. stercoralis* and *S. ratti***
670 A) The life cycle of *S. stercoralis* in a human host [8]. 1) Infection starts when soil-dwelling
671 infective larvae (iL3s) locate a host and skin penetrate. 2) Inside the host, iL3s migrate to the
672 small intestine and develop into reproductively active parasitic females. The eggs and larvae of
673 parasitic females are voided from the host in feces, where they can either develop directly into
674 iL3s (3a) or into non-parasitic "free-living" adults that engage in sexual reproduction (3b). The
675 offspring of the free-living adults all develop into iL3s. Autoinfection can occur when eggs hatch
676 within the host and develop into iL3s.

677 B) The life cycle of *S. ratti* in a rat host [19]. The stages of infection are similar to *S. stercoralis*,
678 with the following differences: a) the progeny of parasitic females leave the host exclusively as
679 unhatched eggs; b) the lack of precocious hatching precludes autoinfection of original hosts.
680
681 **Figure S2: *Strongyloides* free-living males display thermal preferences similar to free-**
682 **living females**
683 A) Individual tracks of *S. stercoralis* free-living males responding to a 20-25°C temperature
684 gradient (T_{start} = 23°C). T_C = 20°C. Each colored line is the track of an individual *S. stercoralis*
685 male's path throughout the 45-minute assay. Black crosses represent the starting positions of
686 each worm. The grey line represents T_{start} = 23°C.
687 B) Individual tracks of *S. ratti* free-living males responding to a temperature gradient from 20°C
688 to 25°C when placed at 23°C. Each colored line is the track of an individual *S. stercoralis* male's
689 path throughout the 45-minute assay. Black crosses represent the starting positions of each
690 worm. The grey bar represents a 1°C-wide starting zone of the assay and is centered on 23°C.
691 C) Quantification of the change in temperature (left) and mean speed (right) for free-living males
692 (FLMs) vs. free-living females (FLFs) of *S. stercoralis* (purple) or *S. ratti* (teal). Icons indicate
693 responses of individual worms, boxes show medians and interquartile ranges, and whiskers
694 show min and max values. *S. stercoralis* FLMs and FLFs migrated similarly in the temperature
695 gradient; *S. ratti* FLMs showed reduced positive thermotaxis relative to *S. ratti* FLFs. The mean
696 speed of worms in the gradient was not significant between the sexes. n = 76 worms for
697 *S. stercoralis* FLFs (7 assays over 5 days), n = 49 worms for *S. stercoralis* FLMs (5 assays over
698 3 days), n = 59 for *S. ratti* FLFs (6 assays over 4 days), and n = 49 for *S. ratti* FLMs (5 assays
699 over 4 days). Icons indicate responses of individual worms, boxes show medians and

700 interquartile ranges, and whiskers show min and max values. ns = not significant, ***p<0.001,
701 two-way ANOVA with Šídák's multiple comparisons test.
702 D) Categorical distribution of thermotaxis behaviors in a ~21-35°C gradient across species.
703 Individuals were considered to have engaged in positive or negative thermotaxis if their position
704 at the end of the assay was outside of a 1 cm neutral exclusion zone centered on the starting
705 position of each individual worm. Individuals that finished the assay within this zone were
706 considered non-responding. ns = not significant, *p<0.05, Fisher's exact test with Bonferroni-
707 Dunn correction for multiple comparisons.
708
709 **Figure S3: *S. stercoralis* FLFs fail to display noxious heat escape behaviors at host body**
710 **temperatures.**
711 A) Individual tracks of *S. stercoralis* free-living females responding to a ~32-40°C temperature
712 gradient (T_{start} = 38°C). T_C = 23°C. Each colored line is the trajectory of an individual worm during
713 the 45-minute assay. Black crosses represent the starting positions of each worm. The grey line
714 represents T_{start} = 38°C.
715 B) Quantification of the change in temperature for *S. stercoralis* free-living females. Values are
716 final temperature – starting temperature for each worm. Icons indicate responses of individual
717 worms; boxes show medians and interquartile ranges; whiskers show min and max values. ns
718 = not significantly different from a hypothetical value of 0, Wilcoxon signed-rank test.
719 C) Categorical distribution of *S. stercoralis* thermotaxis behavior in a ~32-40°C gradient.
720 Individuals were considered to have engaged in positive or negative thermotaxis if their position
721 at the end of the assay was outside of a 1 cm neutral exclusion zone centered on the starting
722 position of each individual worm. Individuals that finished the assay within this zone were
723 considered non-responding.

724

725 **Figure S4: Differences in thermotaxis navigation between *Strongyloides* iL3s and FLFs**

726 A) Tracks of *S. stercoralis* and *S. ratti* iL3s engaging in positive thermotaxis in a ~21-34°C
727 temperature gradient (T_{start} = 30°C, T_C = 23°C). Each colored line is a track of an individual
728 worm's path throughout the 15-minute assay. Black crosses represent the starting positions of
729 each worm. The grey line represents T_{start} = 30°C.

730 B) Quantification of the change in temperature (left), mean speed (center), and distance ratio
731 (right) for *S. stercoralis* iL3s and FLFs (purple), and *S. ratti* iL3s and FLFs (teal). Distance ratio
732 was calculated by dividing the total path length by the distance from starting position to ending
733 position of the assay. A larger distance ratio represents a more circuitous path; a distance ratio
734 of 1 is a completely straight path. Icons indicate responses of individual worms, boxes show
735 medians and interquartile ranges, and whiskers show min and max values. n=30-60 worms from
736 3-6 assays. ns = not significant, ***p<0.001, ****p<0.0001, Kruskal-Wallis test with Dunn's
737 multiple comparisons test.

738

739 **Figure S5: Conditions that elicit negative thermotaxis in *Strongyloides* iL3s do not elicit**
740 **negative thermotaxis in *Strongyloides* FLFs.**

741 A-D) Tracks of *S. stercoralis* iL3s (A), *S. stercoralis* FLFs (B), *S. ratti* iL3s (C), and *S. ratti* FLFs
742 (D) in a ~13-23°C gradient (T_{start} = 20°C, T_C = 23°C). Each colored line is an individual worm's
743 path throughout the 15-minute assay. Black crosses represent the starting positions of each
744 worm. The grey line represents T_{start} = 20°C. Assay duration: 45 minutes (adults) or 15 minutes
745 (iL3s).

746 E) Quantification of the change in temperature experienced by worms in the ~13-23°C gradient.
747 Icons indicate responses of individual worms, boxes show medians and interquartile ranges,

748 and whiskers show min and max values. n = 30-50 worms from 3-5 assays. ***p<0.001,
749 ****p<0.0001, two-way ANOVA with Tukey's multiple comparisons test.
750 F) Categorical distribution of thermotaxis behaviors in a ~13°C-23°C gradient across species.
751 Individuals were considered to have engaged in positive or negative thermotaxis if their position
752 at the end of the assay was above or below 0.5°C of their starting position respectively.
753 Individuals that finished the assay within 0.5°C above or below T_{start} were considered non-
754 responding. ***p<0.001, Fisher's exact test with Bonferroni-Dunn correction for multiple tests.
755
756 **Figure S6: Expanded quantifications of the impact of an attractive odorant on the**
757 **thermotaxis behaviors of *S. stercoralis* FLFs.**
758 A) Tracks of worms in a ~21-25°C pure thermotaxis gradient or a thermal gradient with an
759 attractive odorant (3m1b, pure) placed near (at 22.5°C) or far (at 22°C) from T_{start} (23°C). Assay
760 duration: 45 minutes. Colored tracks represent the path of individual worms. Black crosses
761 represent the starting location of individual worms. The grey line represents T_{start} = 23°C.
762 B) Representative tracks of individual *S. stercoralis* FLFs in each experimental condition from
763 panel A. Tracks are color-coded by time. Vertical red hash lines represent the position of the
764 odorant. Black crosses show the starting location of individual worms.
765 C) Quantification of the minimum temperature experienced by *S. stercoralis* FLFs in a ~21-25°C
766 gradient with and without 3m1b. The minimum temperature experienced in the presence of an
767 odorant was significantly lower than in the temperature-only condition. Icons indicate responses
768 of individual worms, boxes show medians and interquartile ranges, and whiskers show min and
769 max values. ns = not significant, ***p<0.001, ****p<0.0001, Kruskal-Wallis test with Dunn's
770 multiple comparisons test.

771 D) Quantification of the maximum temperature experienced by *S. stercoralis* FLFs in a ~21-25°C
772 gradient with and without 3m1b. The maximum temperature experienced in the presence of an
773 odorant was significantly lower than in the temperature-only condition. n = 76 worms for
774 temperature only (7 assays over 5 days), n = 65 worms for odorant near (6 assays over 3 days),
775 and n = 66 worms for odorant far (6 assays over 3 days). *p<0.05, ****p<0.0001, Kruskal-Wallis
776 test with Dunn's multiple comparisons test.
777 E) Quantification of the starting temperature experienced by *S. stercoralis* FLFs *stercoralis* a
778 ~21-25°C gradient with and without 3m1b. The starting temperatures of worms were not
779 significantly different between the experimental conditions. ns = not significant, Kruskal-Wallis
780 test with Dunn's multiple comparisons test.
781
782 **Figure S7: Kaplan-Meier survival curves for individual experiments.**
783 Probability of survival over time for *C. elegans* adult hermaphrodites, *S. stercoralis* FLFs, and *S.*
784 *ratti* FLFs. Plots show survival curves for independent experiments. n = number of events
785 (number of censored worms). When the number of censored worms is marked with an asterisk
786 (*), the date of censoring is unknown, and the censored worms are excluded from plots and
787 statistical analyses.
788
789 **Figure S8: Impact of environmental temperature on daily brood sizes across species.**
790 **A-C)** Brood size (eggs + larvae) recorded each day for *C. elegans* adults (A), *S. stercoralis* FLFs
791 (B), and *S. ratti* FLFs (C) as a function of incubation temperature. Grey circles = 23°C; yellow
792 diamonds = 30°C; red triangles = 37°C. Icons indicate brood sizes of individual worms, boxes
793 show medians and interquartile ranges, and whiskers show min and max values.

794 **D**) Day one brood size across species. *S. stercoralis* FLFs showed a significant increase in brood
795 size on day 1 of the brood size assay at 30°C and 37°C. *S. ratti* FLFs showed a significant
796 increase in brood size on day 1 of the brood size assay at only 30°C. In contrast, *C. elegans*
797 adults showed a significant decrease in brood size on day 1. n = 31-54 adult worms. ns = not
798 significant, ****p<0.0001, two-way ANOVA with Tukey's multiple comparisons test.

799

800 **Supplemental File 1:** This file includes all data used for statistical analyses and the results of
801 statistical tests, including exact *p* values.

802

803 **References**

804 1. Bethony J, Brooker S, Albonico M, Geiger SM, Loukas A, Diemert D, et al. Soil-transmitted
805 helminth infections: ascariasis, trichuriasis, and hookworm. Lancet. 2006;367: 1521–1532.
806 doi:10.1016/S0140-6736(06)68653-4

807 2. Buonfrate D, Requena-Mendez A, Angheben A, Muñoz J, Gobbi F, Van Den Ende J, et al.
808 Severe strongyloidiasis: a systematic review of case reports. BMC Infect Dis. 2013;13: 78.
809 doi:10.1186/1471-2334-13-78

810 3. Gordon CA, Utzinger J, Muhi S, Becker SL, Keiser J, Khieu V, et al. Strongyloidiasis. Nat
811 Rev Dis Primers. 2024;10: 1–16. doi:10.1038/s41572-023-00490-x

812 4. Schär F, Trostdorf U, Giardina F, Khieu V, Muth S, Marti H, et al. *Strongyloides stercoralis*:
813 global distribution and risk factors. PLoS Negl Trop Dis. 2013;7: e2288.
814 doi:10.1371/journal.pntd.0002288

815 5. Nutman TB. Human infection with *Strongyloides stercoralis* and other related *Strongyloides*
816 species. Parasitology. 2017;144: 263–273. doi:10.1017/S0031182016000834

817 6. Crudo Blackburn C, Yan SM, McCormick D, Herrera LN, Iordanov RB, Bailey MD, et al.
818 Parasitic contamination of soil in the Southern United States. Am J Trop Med Hyg. 2024;
819 tpmd240075. doi:10.4269/ajtmh.24-0075

820 7. Tamarozzi F, Martello E, Giorli G, Fittipaldo A, Staffolani S, Montresor A, et al. Morbidity
821 associated with chronic *Strongyloides stercoralis* infection: a systematic review and meta-
822 analysis. Am J Trop Med Hyg. 2019;100: 1305–1311. doi:10.4269/ajtmh.18-0895

823 8. Viney ME, Lok JB. *Strongyloides* spp. WormBook. 2007; 1–15.
824 doi:10.1895/wormbook.1.141.1

825 9. Page W, Judd JA, Bradbury RS. The unique life cycle of *Strongyloides stercoralis* and
826 implications for public health action. Trop Med Infect Dis. 2018;3.
827 doi:10.3390/tropicalmed3020053

828 10. Beknazarova M, Whiley H, Ross K. Strongyloidiasis: a disease of socioeconomic
829 disadvantage. Int J Environ Res Public Health. 2016;13: 517. doi:10.3390/ijerph13050517

830 11. Fleitas PE, Kehl SD, Lopez W, Travacio M, Nieves E, Gil JF, et al. Mapping the global
831 distribution of *Strongyloides stercoralis* and hookworms by ecological niche modeling.
832 Parasit Vectors. 2022;15: 197. doi:10.1186/s13071-022-05284-w

833 12. Jia T-W, Melville S, Utzinger J, King CH, Zhou X-N. Soil-transmitted helminth reinfection
834 after drug treatment: a systematic review and meta-analysis. Cooper PJ, editor. PLoS
835 Negl Trop Dis. 2012;6: e1621. doi:10.1371/journal.pntd.0001621

836 13. Diawara A, Schwenkenbecher JM, Kaplan RM, Prichard RK. Molecular and biological
837 diagnostic tests for monitoring benzimidazole resistance in human soil-transmitted
838 helminths. Am J Trop Med Hyg. 2013;88: 1052–1061. doi:10.4269/ajtmh.12-0484

839 14. Keiser J, Utzinger J. Efficacy of current drugs against soil-transmitted helminth infections:
840 systematic review and meta-analysis. JAMA. 2008;299: 1937–1948.
841 doi:10.1001/jama.299.16.1937

842 15. Kumar N, Rao TKS, Varghese A, Rathor VS. Internal parasite management in grazing
843 livestock. J Parasit Dis. 2013;37: 151–157. doi:10.1007/s12639-012-0215-z

844 16. Learmount J, Stephens N, Boughtflower V, Barrecheguren A, Rickell K. The development
845 of anthelmintic resistance with best practice control of nematodes on commercial sheep
846 farms in the UK. Vet Parasitol. 2016;229: 9–14. doi:10.1016/j.vetpar.2016.09.006

847 17. Schafer TW, Skopic A. Parasites of the small intestine. Curr Gastroenterol Rep. 2006;8:
848 312–320. doi:10.1007/s11894-006-0052-2

849 18. Lok JB. *Strongyloides stercoralis*: a model for translational research on parasitic
850 nematode biology. WormBook. 2007; 1–18. doi:10.1895/wormbook.1.134.1

851 19. Viney M, Kikuchi T. *Strongyloides ratti* and *S. venezuelensis* - rodent models of
852 *Strongyloides* infection. Parasitology. 2017;144: 285–294.
853 doi:10.1017/S0031182016000020

854 20. Viney ME. Developmental switching in the parasitic nematode *Strongyloides ratti*. Proc
855 Biol Sci. 1996;263: 201–8. doi:10.1098/rspb.1996.0032

856 21. Nolan TJ, Brenes M, Ashton FT, Zhu X, Forbes WM, Boston R, et al. The amphidial
857 neuron pair ALD controls the temperature-sensitive choice of alternative developmental
858 pathways in the parasitic nematode, *Strongyloides stercoralis*. Parasitology. 2004;129:
859 753–759. doi:10.1017/S0031182004006092

860 22. Viney ME, Brown M, Omoding NE, Bailey JW, Gardner MP, Roberts E, et al. Why does
861 HIV infection not lead to disseminated strongyloidiasis? J Infect Dis. 2004;190: 2175–
862 2180. doi:10.1086/425935

863 23. Faust EC, Wells JW, Adams C, Beach TD. The fecundity of parasitic female
864 *Strongyloides*. Proc Soc Exp Biol Med. 1934;31: 1041–1043. doi:10.3181/00379727-31-
865 7431P

866 24. Viney ME, Matthews BE, Walliker D. On the biological and biochemical nature of cloned
867 populations of *Strongyloides ratti*. J Helminthol. 1992;66: 45–52.
868 doi:10.1017/s0022149x00012554

869 25. Cole R, Holroyd N, Tracey A, Berriman M, Viney M. The parasitic nematode *Strongyloides*
870 *ratti* exists predominantly as populations of long-lived asexual lineages. Nat Commun.
871 2023;14: 6427. doi:10.1038/s41467-023-42250-1

872 26. Eberhardt AG, Mayer WE, Streit A. The free-living generation of the nematode
873 *Strongyloides papillosus* undergoes sexual reproduction. Int J Parasitol. 2007;37: 989–
874 1000. doi:10.1016/j.ijpara.2007.01.010

875 27. Grove DI. Human strongyloidiasis. Adv Parasitol. 1996;38: 251–309. doi:10.1016/s0065-
876 308x(08)60036-6

877 28. Streit A. Reproduction in *Strongyloides* (Nematoda): a life between sex and
878 parthenogenesis. Parasitology. 2008;135: 285–294. doi:10.1017/S003118200700399X

879 29. De Ree V, Nath TC, Barua P, Harbecke D, Lee D, Rödelsperger C, et al. Genomic
880 analysis of *Strongyloides stercoralis* and *Strongyloides fuelleborni* in Bangladesh. PLoS
881 Negl Trop Dis. 2024;18: e0012440. doi:10.1371/journal.pntd.0012440

882 30. Schad GA. Morphology and life history of *Strongyloides stercoralis*. In: Grove DI, editor.
883 Strongyloidiasis: a major roundworm infection of man. Taylor & Francis: London, UK;
884 1989. pp. 85–104.

885 31. Al-Jawabreh R, Anderson R, Atkinson LE, Bickford-Smith J, Bradbury RS, Breloer M, et
886 al. *Strongyloides* questions-a research agenda for the future. Philos Trans R Soc Lond B
887 Biol Sci. 2024;379: 20230004. doi:10.1098/rstb.2023.0004

888 32. Hammond MP, Robinson RD. Chromosome complement, gametogenesis, and
889 development of *Strongyloides stercoralis*. J Parasitol. 1994;80: 689. doi:10.2307/3283247

890 33. Castelletto ML, Akimori D, Patel R, Schroeder NE, Hallem EA. Introduction to
891 *Strongyloides stercoralis* anatomy. J Nematol. 2024;56: 20240019. doi:10.2478/jofnem-
892 2024-0019

893 34. Ramot D, MacInnis BL, Lee H-C, Goodman MB. Thermotaxis is a robust mechanism for
894 thermoregulation in *Caenorhabditis elegans* nematodes. J Neurosci. 2008;28: 12546–
895 12557. doi:10.1523/JNEUROSCI.2857-08.2008

35. Hedgecock EM, Russell RL. Normal and mutant thermotaxis in the nematode *Caenorhabditis elegans*. Proc Natl Acad Sci USA. 1975;72: 4061–4065. doi:10.1073/pnas.72.10.4061

36. Garrity PA, Goodman MB, Samuel AD, Sengupta P. Running hot and cold: behavioral strategies, neural circuits, and the molecular machinery for thermotaxis in *C. elegans* and *Drosophila*. Genes Dev. 2010;24: 2365–2382. doi:10.1101/gad.1953710

37. Wittenburg N, Baumeister R. Thermal avoidance in *Caenorhabditis elegans*: an approach to the study of nociception. Proc Natl Acad Sci USA. 1999;96: 10477–10482. doi:10.1073/pnas.96.18.10477

38. Glauser DA, Chen WC, Agin R, Macinnis BL, Hellman AB, Garrity PA, et al. Heat avoidance is regulated by transient receptor potential (TRP) channels and a neuropeptide signaling pathway in *Caenorhabditis elegans*. Genetics. 2011;188: 91–103. doi:10.1534/genetics.111.127100

39. Goodman MB. Thermotaxis navigation behavior. WormBook. 2014; 1–10. doi:10.1895/wormbook.1.168.1

40. Glauser DA. Temperature sensing and context-dependent thermal behavior in nematodes. Curr Opin Neurobiol. 2022;73: 102525. doi:10.1016/j.conb.2022.102525

41. Jurado P, Kodama E, Tanizawa Y, Mori I. Distinct thermal migration behaviors in response to different thermal gradients in *Caenorhabditis elegans*. Genes, Brain and Behavior. 2010;9: 120–127. doi:10.1111/j.1601-183X.2009.00549.x

42. Mohammadi A, Byrne Rodgers J, Kotera I, Ryu WS. Behavioral response of *Caenorhabditis elegans* to localized thermal stimuli. BMC Neurosci. 2013;14: 66. doi:10.1186/1471-2202-14-66

43. Klass MR. Aging in the nematode *Caenorhabditis elegans*: major biological and environmental factors influencing life span. Mech Ageing Dev. 1977;6: 413–429. doi:10.1016/0047-6374(77)90043-4

44. Lithgow GJ, White TM, Hinerfeld DA, Johnson TE. Thermotolerance of a long-lived mutant of *Caenorhabditis elegans*. J Gerontol. 1994;49: B270–B276. doi:10.1093/geronj/49.6.B270

45. Hirsh D, Oppenheim D, Klass M. Development of the reproductive system of *Caenorhabditis elegans*. Dev Biol. 1976;49: 200–219. doi:10.1016/0012-1606(76)90267-0

46. Petrella LN. Natural variants of *C. elegans* demonstrate defects in both sperm function and oogenesis at elevated temperatures. PLOS ONE. 2014;9: e112377. doi:10.1371/journal.pone.0112377

47. McMullen PD, Aprison EZ, Winter PB, Amaral LAN, Morimoto RI, Ruvinsky I. Macro-level modeling of the response of *C. elegans* reproduction to chronic heat stress. PLoS Comput Biol. 2012;8: e1002338. doi:10.1371/journal.pcbi.1002338

933 48. Harvey SC, Viney ME. Thermal variation reveals natural variation between isolates of
934 *Caenorhabditis elegans*. J Exp Zool Pt B Mol Dev Evol. 2007;308B: 409–416.
935 doi:10.1002/jez.b.21161

936 49. Begasse ML, Leaver M, Vazquez F, Grill SW, Hyman AA. Temperature dependence of
937 cell division timing accounts for a shift in the thermal limits of *C. elegans* and *C. briggsae*.
938 Cell Rep. 2015;10: 647–653. doi:10.1016/j.celrep.2015.01.006

939 50. Lee S-J, Kenyon C. Regulation of the longevity response to temperature by
940 thermosensory neurons in *Caenorhabditis elegans*. Curr Biol. 2009;19: 715–722.
941 doi:10.1016/j.cub.2009.03.041

942 51. Bryant AS, Hallem EA. Terror in the dirt: Sensory determinants of host seeking in soil-
943 transmitted mammalian-parasitic nematodes. Int J Parasitol Drugs Drug Resist. 2018;8:
944 496–510. doi:10.1016/j.ijpddr.2018.10.008

945 52. Banerjee N, Gang SS, Castelletto ML, Ruiz F, Hallem EA. Carbon dioxide shapes
946 parasite-host interactions in a human-infective nematode. bioRxiv; 2024.
947 doi:10.1101/2024.03.28.587273

948 53. Gang SS, Castelletto ML, Yang E, Ruiz F, Brown TM, Bryant AS, et al. Chemosensory
949 mechanisms of host seeking and infectivity in skin-penetrating nematodes. Proc Natl Acad
950 Sci USA. 2020;117: 17913–17923. doi:10.1073/pnas.1909710117

951 54. Bryant AS, Hallem EA. Temperature-dependent behaviors of parasitic helminths. Neurosci
952 Lett. 2018;687: 290–303. doi:10.1016/j.neulet.2018.10.023

953 55. Bryant AS, Ruiz F, Gang SS, Castelletto ML, Lopez JB, Hallem EA. A critical role for
954 thermosensation in host seeking by skin-penetrating nematodes. Curr Biol. 2018;28:
955 2338–2347. doi:10.1016/j.cub.2018.05.063

956 56. Bryant AS, Ruiz F, Lee JH, Hallem EA. The neural basis of heat seeking in a human-
957 infective parasitic worm. Curr Biol. 2022;32: 2206-2221.e6. doi:10.1016/j.cub.2022.04.010

958 57. Castelletto ML, Gang SS, Okubo RP, Tselikova AA, Nolan TJ, Platzer EG, et al. Diverse
959 host-seeking behaviors of skin-penetrating nematodes. PLoS Pathog. 2014;10:
960 e1004305. doi:10.1371/journal.ppat.1004305

961 58. Castelletto ML, Hallem EA. Generating transgenics and knockouts in *Strongyloides*
962 species by microinjection. JoVE. 2021; 63023. doi:10.3791/63023

963 59. Hawdon JM, Schad GA. Long-term storage of hookworm infective larvae in buffered
964 saline solution maintains larval responsiveness to host signals. J Helm Soc Wash.
965 1991;58: 140–142.

966 60. Stiernagle T. Maintenance of *C. elegans*. WormBook. 2006; 1–11,
967 http://www.wormbook.org. doi:10.1895/wormbook.1.101.1

968 61. Schindelin J, Arganda-Carreras I, Frise E, Kaynig V, Longair M, Pietzsch T, et al. Fiji: an
969 open-source platform for biological-image analysis. Nat Methods. 2012;9: 676–682.
970 doi:10.1038/nmeth.2019

971 62. Han SK, Lee D, Lee H, Kim D, Son HG, Yang J-S, et al. OASIS 2: online application for
972 survival analysis 2 with features for the analysis of maximal lifespan and healthspan in
973 aging research. Oncotarget. 2016;7: 56147–56152. doi:10.18632/oncotarget.11269

974 63. Kang H. Sample size determination and power analysis using the G*Power software. J
975 Educ Eval Health Prof. 2021;18: 17. doi:10.3352/jeehp.2021.18.17

976 64. Glauser DA. How and why *Caenorhabditis elegans* uses distinct escape and avoidance
977 regimes to minimize exposure to noxious heat. Worm. 2013;2: e27285.
978 doi:10.4161/worm.27285

979 65. Schild LC, Glauser DA. Dynamic switching between escape and avoidance regimes
980 reduces *Caenorhabditis elegans* exposure to noxious heat. Nat Commun. 2013;4: 2198.
981 doi:10.1038/ncomms3198

982 66. Ghosh R, Mohammadi A, Kruglyak L, Ryu WS. Multiparameter behavioral profiling reveals
983 distinct thermal response regimes in *Caenorhabditis elegans*. BMC Biology. 2012;10: 85.
984 doi:10.1186/1741-7007-10-85

985 67. Takeishi A, Takagaki N, Kuhara A. Temperature signaling underlying thermotaxis and cold
986 tolerance in *Caenorhabditis elegans*. J Neurogenet. 2020;34: 351–362.
987 doi:10.1080/01677063.2020.1734001

988 68. Xiao R, Xu XZS. Temperature sensation: from molecular thermosensors to neural circuits
989 and coding principles. Annu Rev Physiol. 2021;83: 205–230. doi:10.1146/annurev-
990 physiol-031220-095215

991 69. Mendez P, Walsh B, Hallem EA. Using newly optimized genetic tools to probe
992 *Strongyloides* sensory behaviors. Mol Biochem Parasitol. 2022;250: 111491.
993 doi:10.1016/j.molbiopara.2022.111491

994 70. Fisher MC, Viney ME. The population genetic structure of the facultatively sexual parasitic
995 nematode *Strongyloides ratti* in wild rats. Proc Biol Sci. 1998;265: 703–709.
996 doi:10.1098/rspb.1998.0350

997 71. Richards JL, Zacharias AL, Walton T, Burdick JT, Murray JI. A quantitative model of
998 normal *Caenorhabditis elegans* embryogenesis and its disruption after stress. Dev Biol.
999 2013;374: 12–23. doi:10.1016/j.ydbio.2012.11.034

1000 72. Neves A, Busso C, Gönczy P. Cellular hallmarks reveal restricted aerobic metabolism at
1001 thermal limits. eLife. 2024;4: e04810. doi:10.7554/eLife.04810

1002 73. Plagens RN, Mossiah I, Kim Guisbert KS, Guisbert E. Chronic temperature stress inhibits
1003 reproduction and disrupts endocytosis via chaperone titration in *Caenorhabditis elegans*.
1004 BMC Biol. 2021;19: 75. doi:10.1186/s12915-021-01008-1

1005 74. Aprison EZ, Ruvinsky I. Balanced trade-offs between alternative strategies shape the
1006 response of *C. elegans* reproduction to chronic heat stress. PLoS One. 2014;9: e105513.
1007 doi:10.1371/journal.pone.0105513

1008 75. Banerjee N, Shih P-Y, Rojas Palato EJ, Sternberg PW, Hallem EA. Differential processing
1009 of a chemosensory cue across life stages sharing the same valence state in
1010 *Caenorhabditis elegans*. Proc Natl Acad Sci U S A. 2023;120: e2218023120.
1011 doi:10.1073/pnas.2218023120

1012 76. Rengarajan S, Yankura KA, Guillermin ML, Fung W, Hallem EA. Feeding state sculpts a
1013 circuit for sensory valence in *Caenorhabditis elegans*. Proc Natl Acad Sci U S A.
1014 2019;116: 1776–1781. doi:10.1073/pnas.1807454116

1015 77. Grove DI, Heenan PJ, Northern C. Persistent and disseminated infections with
1016 *Strongyloides stercoralis* in immunosuppressed dogs. Int J Parasitol. 1983;13: 483–490.
1017 doi:10.1016/S0020-7519(83)80012-5

1018 78. Gardner MP, Gems D, Viney ME. Extraordinary plasticity in aging in *Strongyloides ratti*
1019 implies a gene-regulatory mechanism of lifespan evolution. Aging Cell. 2006;5: 315–323.
1020 doi:10.1111/j.1474-9726.2006.00226.x

1021 79. Patel R, Bryant AS, Castelletto ML, Walsh B, Akimori D, Hallem EA. The generation of
1022 stable transgenic lines in the human-infective nematode *Strongyloides stercoralis*. G3
1023 (Bethesda). 2024; jkae122. doi:10.1093/g3journal/jkae122

1024 80. Grant WN, Stasiuk S, Newton-Howes J, Ralston M, Bisset SA, Heath DD, et al.
1025 *Parastrongyloides trichosuri*, a nematode parasite of mammals that is uniquely suited to
1026 genetic analysis. Int J Parasitol. 2006;36: 453–466. doi:10.1016/j.ijpara.2005.11.009

1027 81. Udonsi JK, Atata G. *Necator americanus*: temperature, pH, light, and larval development,
1028 longevity, and desiccation tolerance. Exp Parasitol. 1987;63: 136–142. doi:10.1016/0014-
1029 4894(87)90154-8

1030 82. Smith G, Schad GA. *Ancylostoma duodenale* and *Necator americanus*: effect of
1031 temperature on egg development and mortality. Parasitology. 1989;99: 127–132.
1032 doi:10.1017/s0031182000061102

1033 83. Arene FOI. *Ascaris suum*: Influence of embryonation temperature on the viability of the
1034 infective larva. Journal of Thermal Biology. 1986;11: 9–15. doi:10.1016/0306-
1035 4565(86)90011-2

1036 84. Senecal J, Nordin A, Vinnerås B. Fate of *Ascaris* at various pH, temperature and moisture
1037 levels. J Water Health. 2020;18: 375–382. doi:10.2166/wh.2020.264

1038 85. Naidoo D, Foutch GL. The time-temperature relationship for the inactivation of *Ascaris*
1039 eggs. J Water Sanit Hyg Dev. 2017;8: 123–126. doi:10.2166/washdev.2017.102

1040 86. Harroff LA, Liotta JL, Bowman DD, Angenent LT. Current time-temperature relationships
1041 for thermal inactivation of *Ascaris* eggs at mesophilic temperatures are too conservative

1042 and may hamper development of simple, but effective sanitation. Water Res X. 2019;5:
1043 100036. doi:10.1016/j.wroa.2019.100036

1044 87. Maya C, Torner-Morales FJ, Lucario ES, Hernández E, Jiménez B. Viability of six species
1045 of larval and non-larval helminth eggs for different conditions of temperature, pH and
1046 dryness. Water Res. 2012;46: 4770–4782. doi:10.1016/j.watres.2012.06.014

1047 88. Barrett J. The effect of temperature on the development and survival of the infective
1048 larvae of *Strongyloides ratti* Sandground, 1925. Parasitology. 1968;58: 641–651.
1049 doi:10.1017/S0031182000028936

1050 89. Fenton A, Paterson S, Viney ME, Gardner MP. Determining the optimal developmental
1051 route of *Strongyloides ratti*: an evolutionarily stable strategy approach. Evolution. 2004;58:
1052 989–1000. doi:10.1111/j.0014-3820.2004.tb00433.x

1053 90. Vanalli C, Mari L, Casagrandi R, Gatto M, Cattadori IM. Helminth ecological requirements
1054 shape the impact of climate change on the hazard of infection. Ecol Lett. 2024;27:
1055 e14386. doi:10.1111/ele.14386

1056 91. Blum AJ, Hotez PJ. Global “worming”: Climate change and its projected general impact on
1057 human helminth infections. Liang S, editor. PLoS Negl Trop Dis. 2018;12: e0006370.
1058 doi:10.1371/journal.pntd.0006370

1059 92. Okulewicz A. The impact of global climate change on the spread of parasitic nematodes.
1060 Ann Parasitol. 2017;63: 15–20. doi:10.17420/ap6301.79

1061

Figure 1

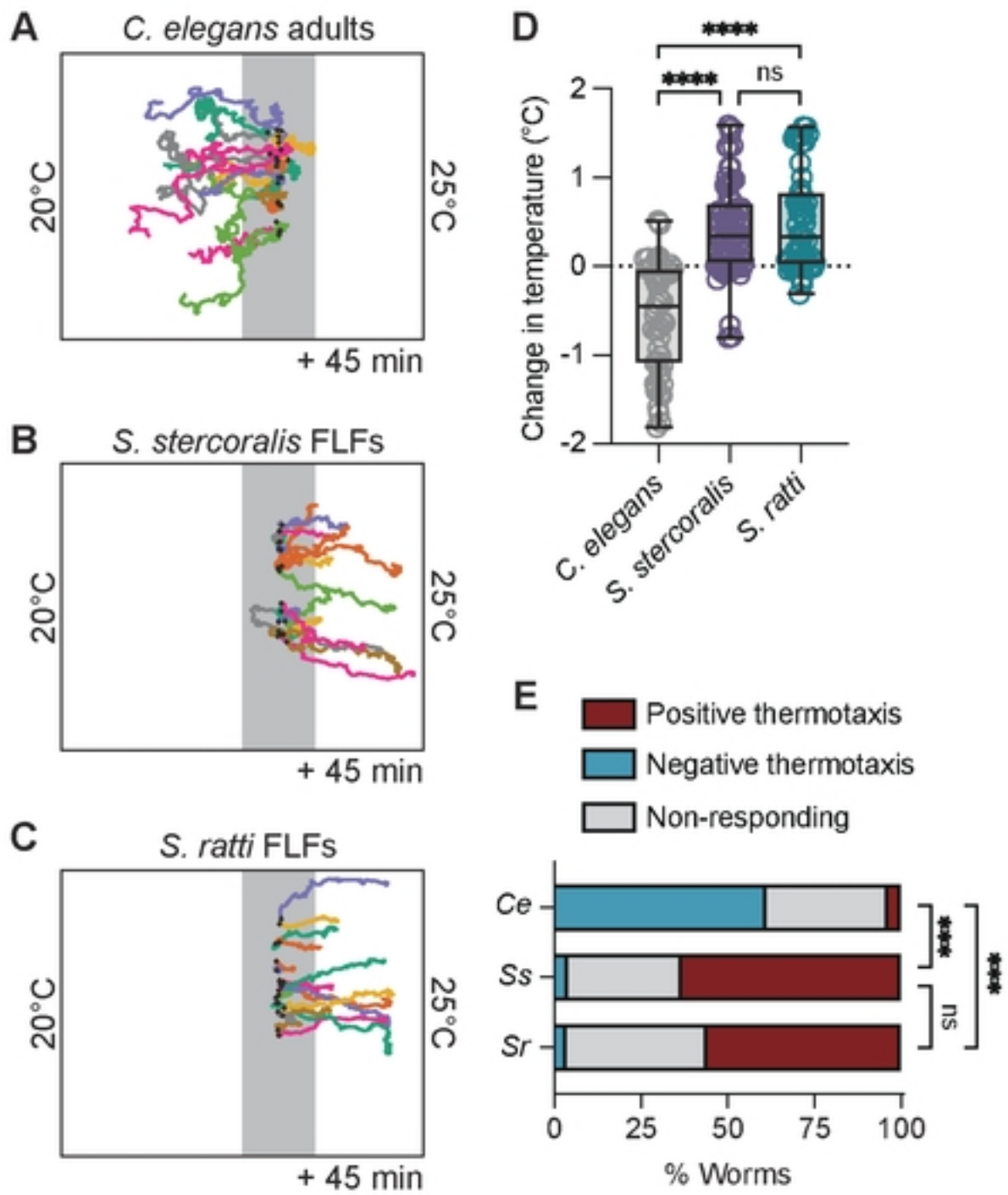
A
C. elegans adults
20°C
25°C
+ 45 min
B
S. stercoralis FLFs
20°C
25°C
+ 45 min
C
S. ratti FLFs
20°C
25°C
+ 45 min
D
****
****
ns
Change in temperature (°C)
2
1
0
-1
-2
C. elegans
S. stercoralis
S. ratti
E
Positive thermotaxis
Negative thermotaxis
Non-responding
Ce
Ss
Sr
***
ns
***
0
25
50
75
100
% Worms

Figure 2

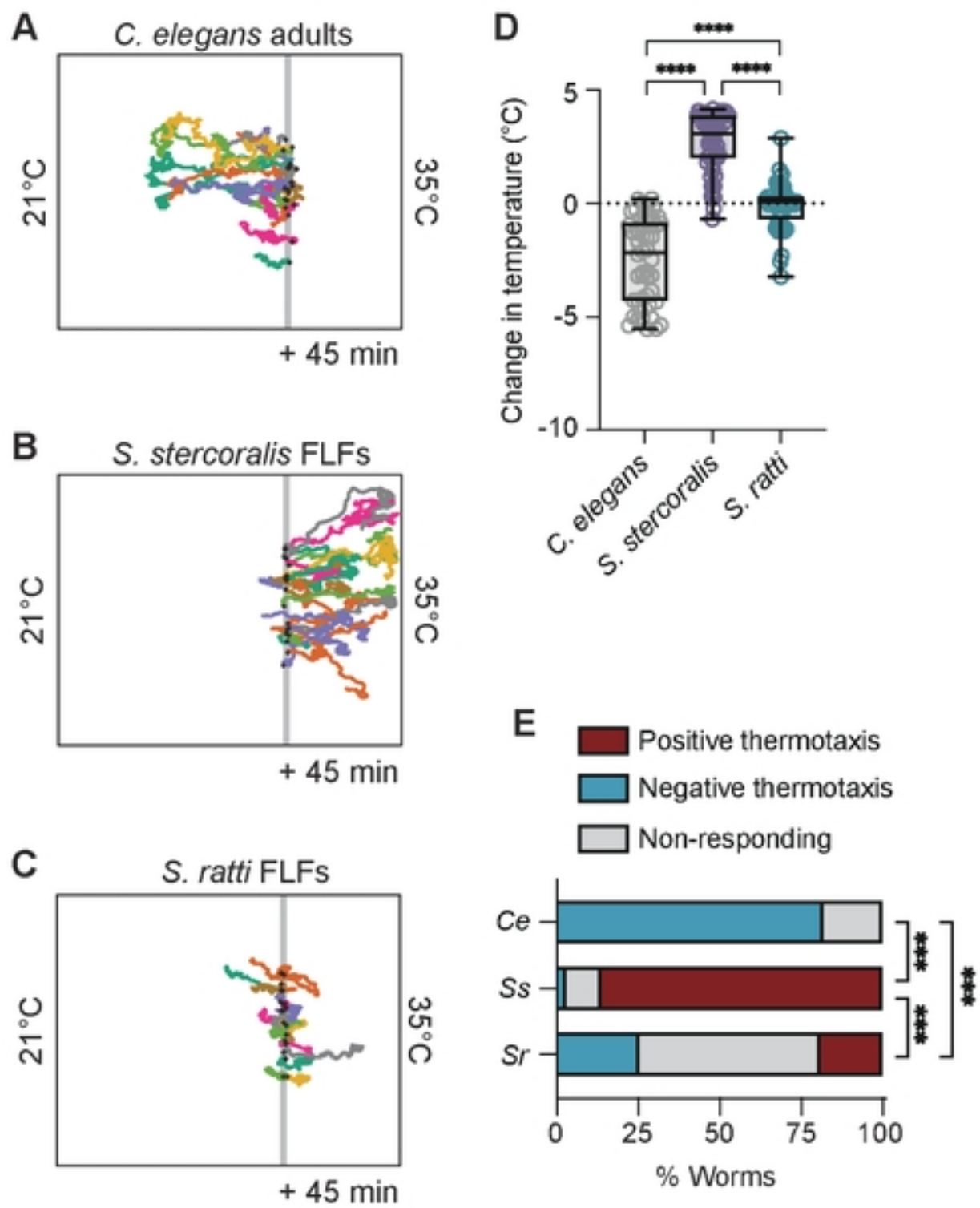
A
C. elegans adults
21°C
35°C
+ 45 min
B
S. stercoralis FLFs
21°C
35°C
+ 45 min
C
S. ratti FLFs
21°C
35°C
+ 45 min
D
Change in temperature (°C)
5
0
-5
-10
****
****
****
C. elegans
S. stercoralis
S. ratti
E
Positive thermotaxis
Negative thermotaxis
Non-responding
Ce
Ss
Sr
***
***
***
0
25
50
75
100
% Worms

Figure 3

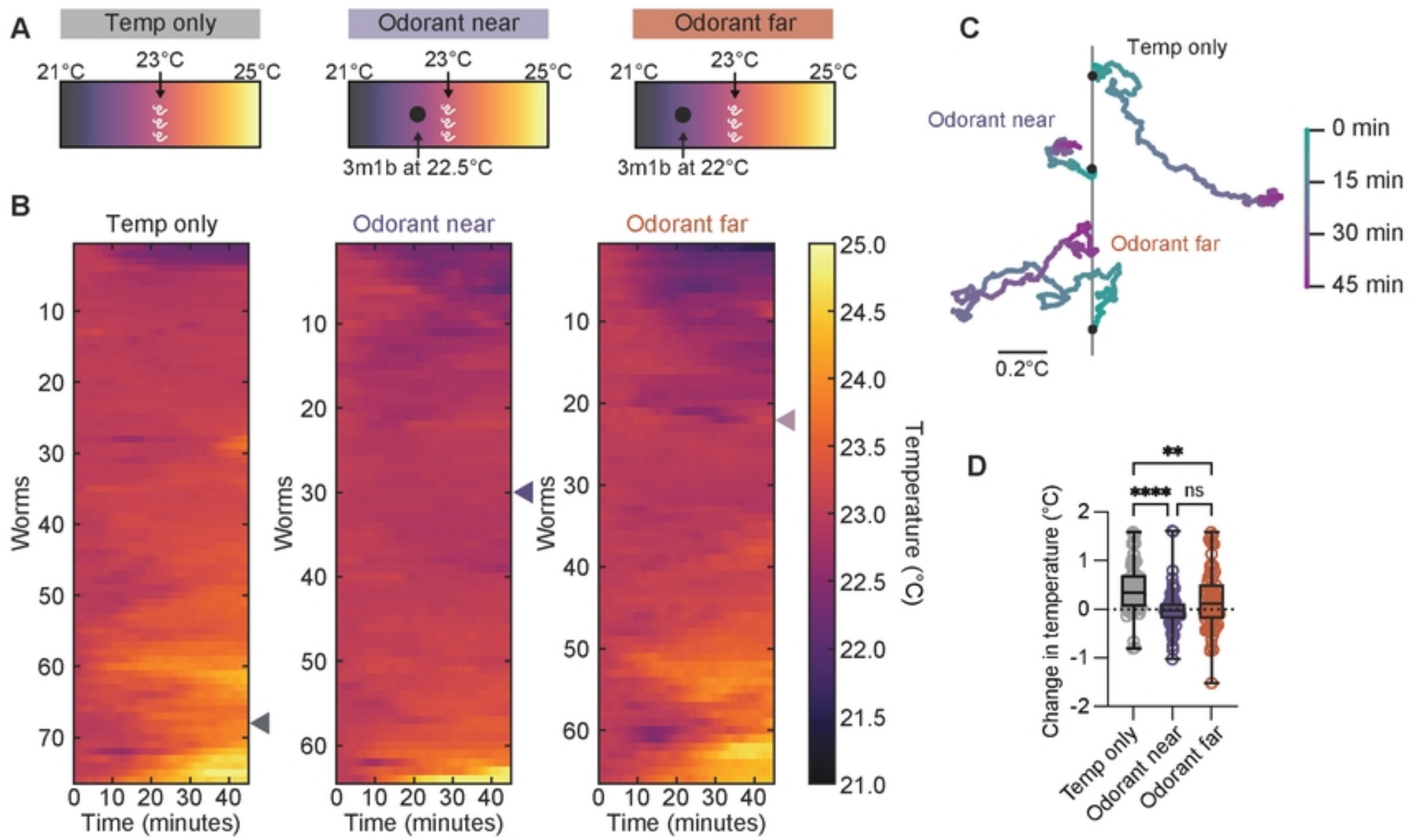
A
Temp only
Odorant near
Odorant far
21°C
23°C
25°C
3m1b at 22.5°C
3m1b at 22°C
B
Temp only
Odorant near
Odorant far
Worms
Time (minutes)
Temperature (°C)
C
Temp only
Odorant near
Odorant far
0 min
15 min
30 min
45 min
0.2°C
D
Change in temperature (°C)
Temp only
Odorant near
Odorant far
**
****
ns

Figure 4

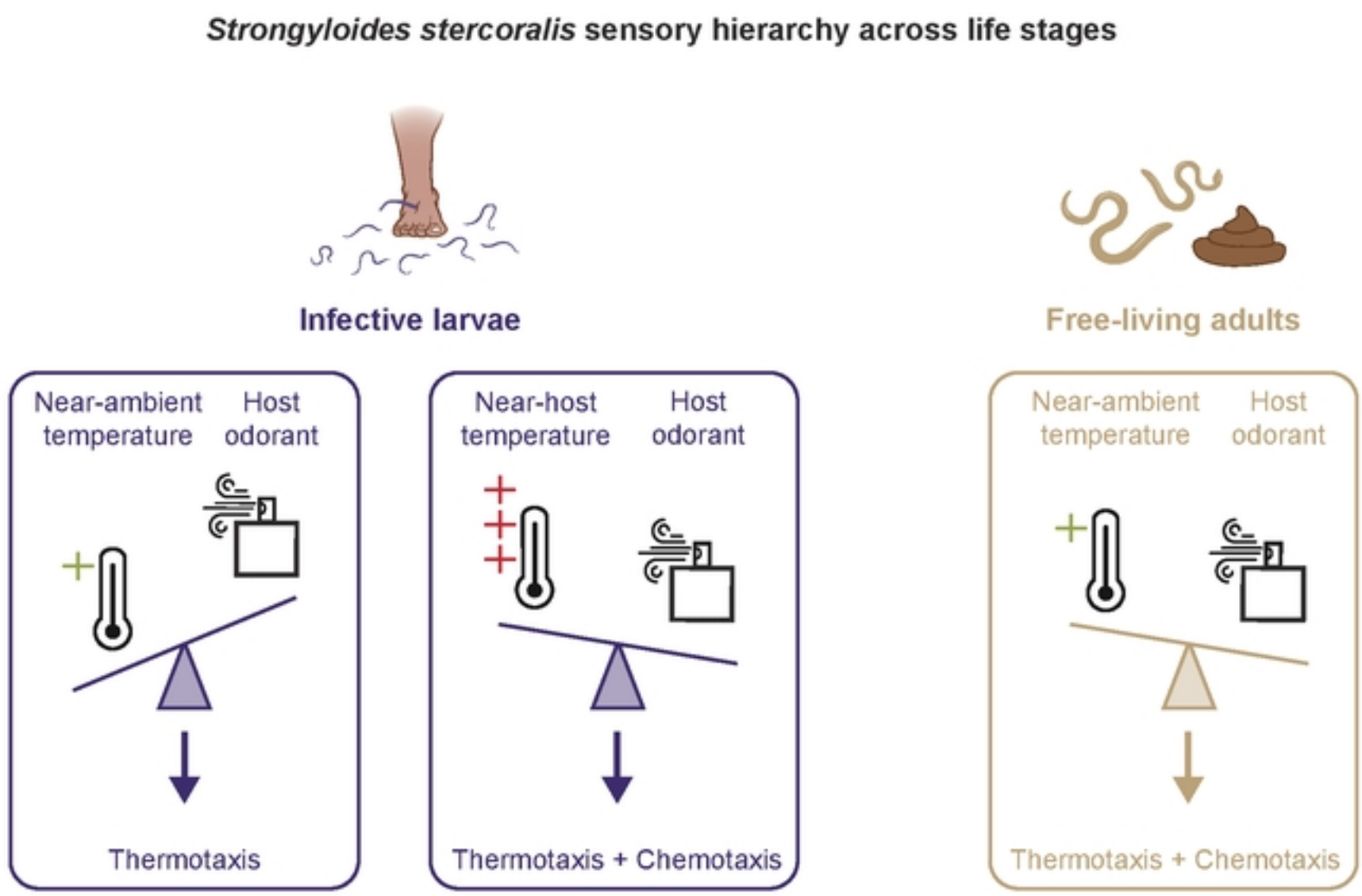
Strongyloides stercoralis sensory hierarchy across life stages
Infective larvae
Free-living adults
Near-ambient temperature
Host odorant
Thermotaxis
Near-host temperature
Host odorant
Thermotaxis + Chemotaxis
Near-ambient temperature
Host odorant
Thermotaxis + Chemotaxis

Figure 5

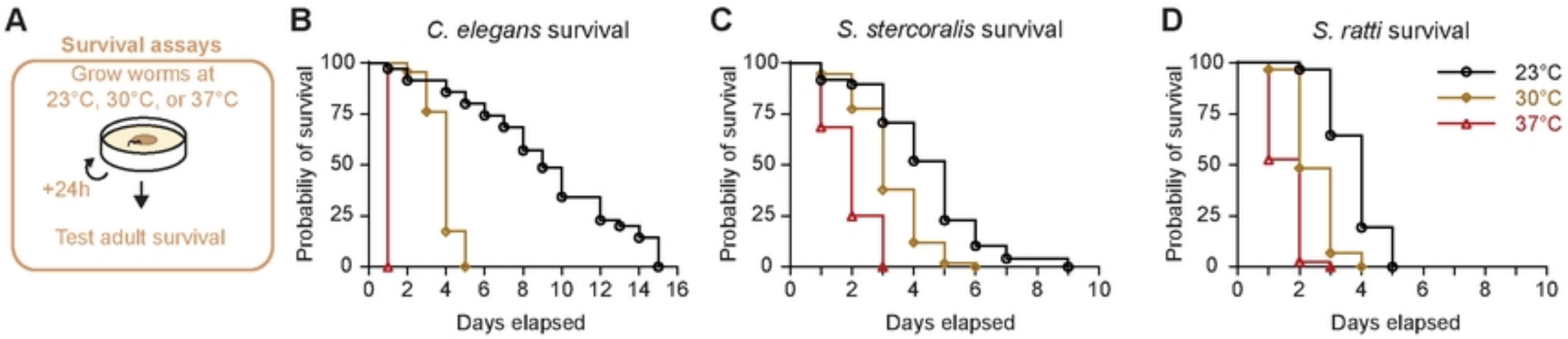

E

Mean Survival (days)

Growth Temperature	*C. elegans* mean ± SE (n)	*S. stercoralis* mean ± SE (n)	*S. ratti* mean ± SE (n)
23°C	9.2 ± 0.68 (35)	4.47 ± 0.26 (51)	3.84 ± 0.14 (35)
30°C	3.89 ± 0.11 (46)***	3.25 ± 0.15 (56)***	2.59 ± 0.13 (34)***
37°C	1 ± 0.0 (40)***	1.96 ± 0.11 (51)***	1.71 ± 0.11 (44)***

Figure 6

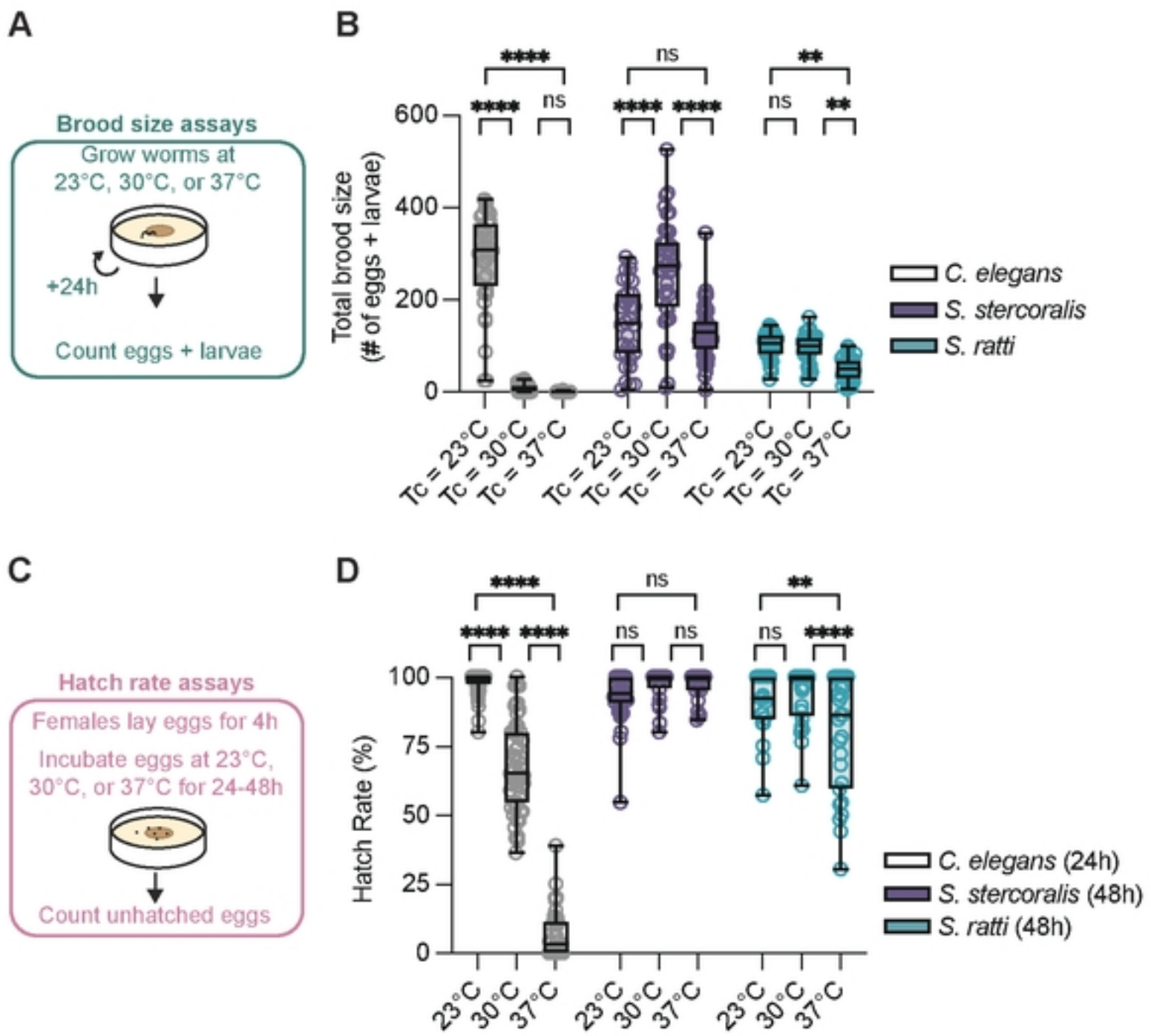
A
Brood size assays
Grow worms at
23°C, 30°C, or 37°C
+24h
Count eggs + larvae
B
Total brood size
(# of eggs + larvae)
600
400
200
0
****
ns
****
****
ns
**
Tc = 23°C
Tc = 30°C
Tc = 37°C
C. elegans
S. stercoralis
S. ratti
C
Hatch rate assays
Females lay eggs for 4h
Incubate eggs at 23°C,
30°C, or 37°C for 24-48h
Count unhatched eggs
D
Hatch Rate (%)
100
75
50
25
0
23°C
30°C
37°C
C. elegans (24h)
S. stercoralis (48h)
S. ratti (48h)

Figure 7

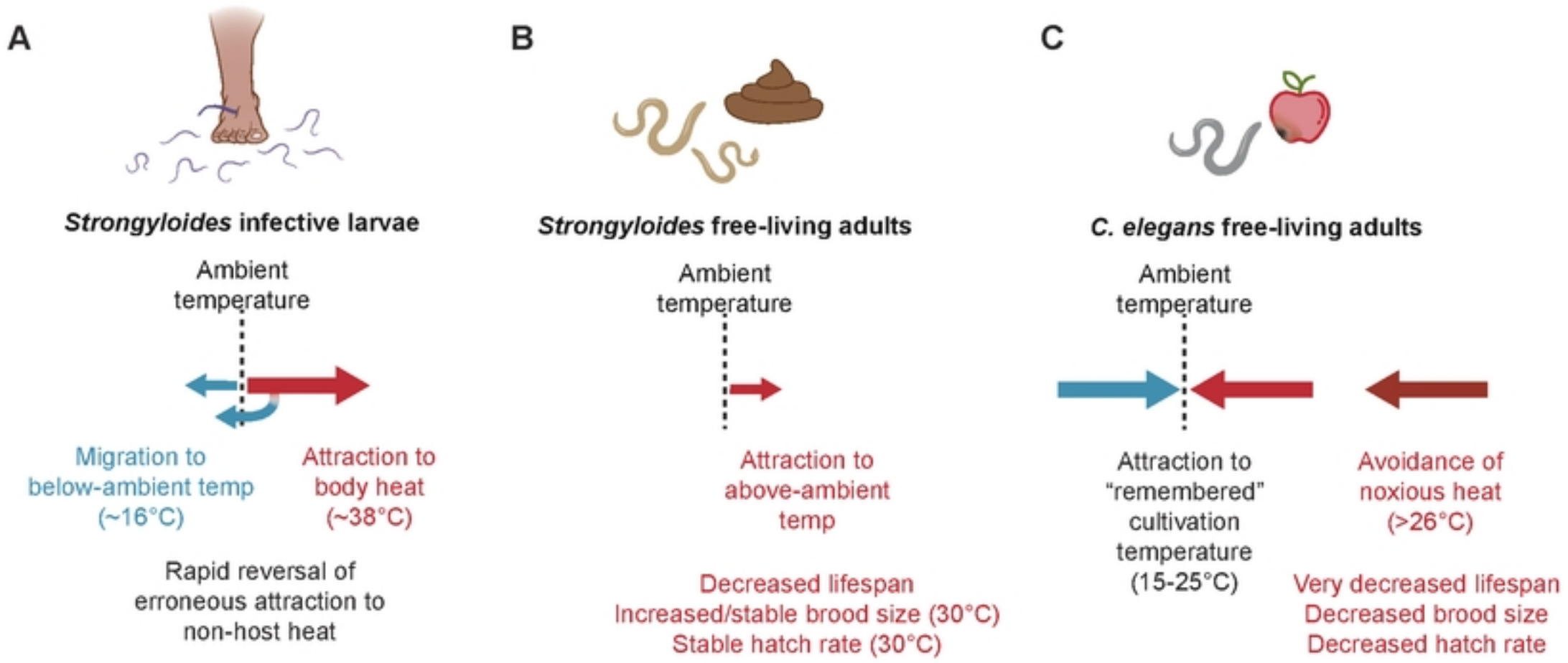
A
Strongyloides infective larvae
Ambient temperature
Migration to below-ambient temp (~16°C)
Attraction to body heat (~38°C)
Rapid reversal of erroneous attraction to non-host heat
B
Strongyloides free-living adults
Ambient temperature
Attraction to above-ambient temp
Decreased lifespan
Increased/stable brood size (30°C)
Stable hatch rate (30°C)
C
C. elegans free-living adults
Ambient temperature
Attraction to "remembered" cultivation temperature (15-25°C)
Avoidance of noxious heat (>26°C)
Very decreased lifespan
Decreased brood size
Decreased hatch rate